AD-A161 431 ANALYSIS OF PULSE PROPAGATION IN COUPLED MICROSTRIP TRANSMISSION LINES(U) ILLINOIS UNIV AT URBANA COORDINATED SCIENCE LAB J E SCHUTT-AINE ET AL MAR 85 1/1

UNCLASSIFIED R-1036 N00014-84-C-0149 F/G 9/5 NL

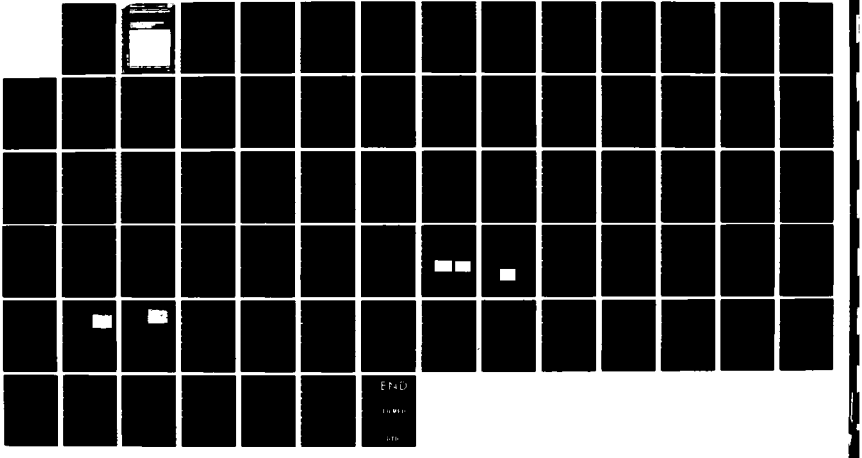

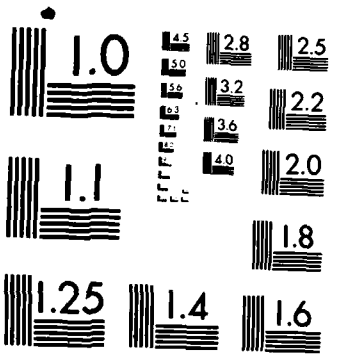

MICROCOPY RESOLUTION TEST CHART
NATIONAL BUREAU OF STANDARDS-1963-A

AD-A161 431

Unclassified

SECURITY CLASSIFICATION OF THIS PAGE

REPORT DOCUMENTATION PAGE

1a. REPORT SECURITY CLASSIFICATION Unclassified	1b. RESTRICTIVE MARKINGS None
2a. SECURITY CLASSIFICATION AUTHORITY N/A	3. DISTRIBUTION/AVAILABILITY OF REPORT Approved for public release, distribution unlimited.
2b. DECLASSIFICATION/DOWNGRADING SCHEDULE N/A	
4. PERFORMING ORGANIZATION REPORT NUMBER(S) R-report #1036	5. MONITORING ORGANIZATION REPORT NUMBER(S) N/A
6a. NAME OF PERFORMING ORGANIZATION Coordinated Science Lab Univ. of Illinois 6b. OFFICE SYMBOL (If applicable) N/A	7a. NAME OF MONITORING ORGANIZATION Office of Naval Research
6c. ADDRESS (City, State and ZIP Code) 1101 W. Springfield Avenue Urbana, Illinois 61801	7b. ADDRESS (City, State and ZIP Code) 800 N. Quincy Street Arlington, VA 22217
8a. NAME OF FUNDING/SPONSORING ORGANIZATION 8b. OFFICE SYMBOL (If applicable) N/A	9. PROCUREMENT INSTRUMENT IDENTIFICATION NUMBER Contract #N00014-84-C-0149
8c. ADDRESS (City, State and ZIP Code)	10. SOURCE OF FUNDING NOS. PROGRAM ELEMENT NO. / PROJECT NO. / TASK NO. / WORK UNIT NO.
11. TITLE (Include Security Classification) Analysis of Pulse propagation in coupled microstrip transmission line	
12. PERSONAL AUTHOR(S) J. E. Schutt-aine and R. Mittra	
13a. TYPE OF REPORT Technical 13b. TIME COVERED FROM _____ TO _____	14. DATE OF REPORT (Yr., Mo., Day) March 1985 15. PAGE COUNT
16. SUPPLEMENTARY NOTATION N/A	
17. COSATI CODES FIELD / GROUP / SUB. GR.	18. SUBJECT TERMS (Continue on reverse if necessary and identify by block number) High speed Digital Circuits; Pulse Propagation; Coupled Microstrip Lines; Cross Talk

19. ABSTRACT (Continue on reverse if necessary and identify by block number)

In this report the problem of propagation of high speed pulses is considered. The purpose of this analysis is to investigate effects such as RC delays, reflection cross-coupling or cross talk, etc. in coupled microstrip lines. Two-, three-, and coupled N-line configurations are considered under various conditions of terminations.

20. DISTRIBUTION/AVAILABILITY OF ABSTRACT UNCLASSIFIED/UNLIMITED ☒ SAME AS RPT. ☐ DTIC USERS ☐	21. ABSTRACT SECURITY CLASSIFICATION Unclassified
22a. NAME OF RESPONSIBLE INDIVIDUAL	22b. TELEPHONE NUMBER (Include Area Code) 22c. OFFICE SYMBOL None

DD FORM 1473, 83 APR EDITION OF 1 JAN 73 IS OBSOLETE.

Unclassified

SECURITY CLASSIFICATION OF THIS PAGE

ANALYSIS OF PULSE PROPAGATION IN COUPLED MICROSTRIP TRANSMISSION LINES

BY

J. E. Schutt-Aine and R. Mittra

Department of Electrical & Computer Engineering
University of Illinois
Urbana, Illinois

The work reported in this paper was supported in part by the Joint Services Electronics Program, N00014-84-C-0149.

TABLE OF CONTENTS

CHAPTER 1

INTRODUCTION

High speed digital circuits have resulted from the miniaturization of solid-state devices and the implementation of those circuits into dense systems (VLSI and VHSI). Switching devices presently used have rise times and pulse widths in the range of a few nanoseconds. Moreover, devices with switching delays of less than 10 picoseconds are being developed from which delays of less than 50 picoseconds will probably result in large computers. Aside from the physical characteristics of the devices, interconnections are another parameter which determine the speed of these systems. Today, interconnections represent the main limiting factor in the reduction of speed because of the inevitable RC delay they introduce. Moreover, with increased density and speed, the problem of cross-coupling has become more critical since noise resulting from unwanted signals must be limited. Finally, reflections at the terminals due to mismatch along with device nonlinearities, contribute to the complications which have posed some severe constraints for switching network design.

In this study, the problems associated with the propagation of fast pulses in microstrip interconnections will be analyzed. The purpose of this analysis is to investigate each effect such as RC delay, reflections, cross-coupling, nonlinearities, and to propose a model for the combined effect. Such a model is essential since it provides the engineer with the necessary elements from which design guidelines can be implemented while giving a better understanding of noise phenomenon.

In order to develop the model, it will be necessary to determine the physical characteristics of the interconnections as well as those of the propagation medium. Unfortunately, analytical expressions predicting those physical characteristics are not always realistic and do not account for processing variations, nor can they be applied to arbitrary geometries. To

circumvent this obstacle, several measurement techniques will have to be developed in order to obtain the important physical parameters.

An overview of the presently available microstrip technology along with the theoretical foundations is first explained. Some techniques of measurements in the time domain and in the frequency domain are then discussed for both single and coupled lines. Experimental results are finally analyzed and extensions to multiple lines are attempted.

1.1 Characteristics of Microtrip Transmission Lines

Numerous investigators have studied the properties of microstrip transmission lines , proposed models, design equations, and various approaches for the analysis. Figure 1.1 shows a cross section of a microstrip line which consists of a strip conductor of width W resting on a substrate of thickness h and dielectric constant ϵ_r , and a ground plane which serves as the return path. The conductor can be either copper, gold, or an alloy of tin and nickel.

Since the fields between the strip and the ground plane are not entirely within the substrate, the propagating mode along the strip is not purely tranverse electromagnectic (TEM) but quasi-TEM with a phase velocity v_o given by

$$v_o = \frac{c}{\sqrt{\epsilon_e}} \tag{1.1}$$

where c is the speed of light in vacuum and ϵ_e , the effective dielectric constant of the substrate. The wavelength λ_m in the line is :

$$\lambda_m = \frac{v_o}{f} \tag{1.2}$$

where f is the frequency of the propagating signal. Moreover, if the line is assumed to be lossless its characteristic impedance (or wave impedance) Z_m , is expressed by

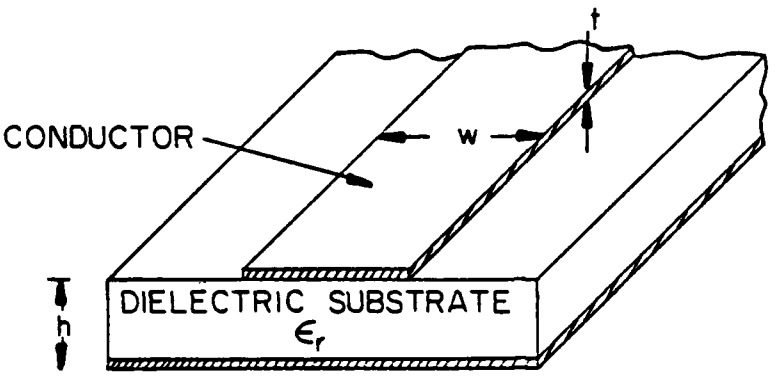

h = SUBSTRATE THICKNESS
t = STRIP CONDUCTOR THICKNESS
w = STRIP CONDUCTOR WIDTH
ϵ_r = DIELECTRIC CONSTANT

(a) CROSS SECTION OF MICROSTRIP LINE

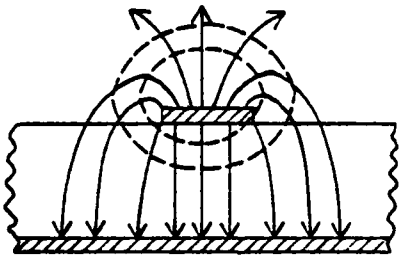

——— ELECTRIC FIELD LINES
- - - - - MAGNETIC FIELD LINES

(b) FIELD CONFIGURATION

Figure 1.1 : Microstrip transmission line: (a) cross section showing the geometric parameters ; (b) field lines. Since all the lines do not pass through the dielectric, a quasi-TEM analysis must be used.

$$Z_o = \sqrt{\frac{L_s}{C_s}} \tag{1.3}$$

where L_s and C_s are the self-inductance and self-capacitance per unit length, respectively. From Maxwell's equations it can be shown that Z_o and v_o are related by

$$Z_o = \frac{1}{v_o c} \tag{1.4}$$

At lower microwave frequencies, the quasi-TEM model can be shown to be fairly accurate. At higher frequencies a hybrid mode analysis would be required. This analysis is far more rigorous, and we will restrain ourselves to the frequency range where the quasi-TEM model is valid.

1.2 Close Form Expressions and Design Equation

Based on the quasi-TEM model, several techniques for characterizing microstrip transmission lines have been proposed. These techniques include conformal mapping [1], [2], the method of Green's functions [3], [4], [5], the moment method [6], and variational techniques [7], [8]. Close form expressions from Wheeler [2], Schneider [9], and Hammerstad [10] have been reported. They contain useful relationships between the effective dielectric constant, the physical dimensions and the electrical parameters of the line. For instance, Hammerstad's equations give the width to height ratio as a function of the desired characteristic impedance (Figure 1.2).

For $W/h \leqslant =2$,

$$\frac{W}{h} = \frac{8\exp(A)}{\exp(2A) - 2} \tag{1.5}$$

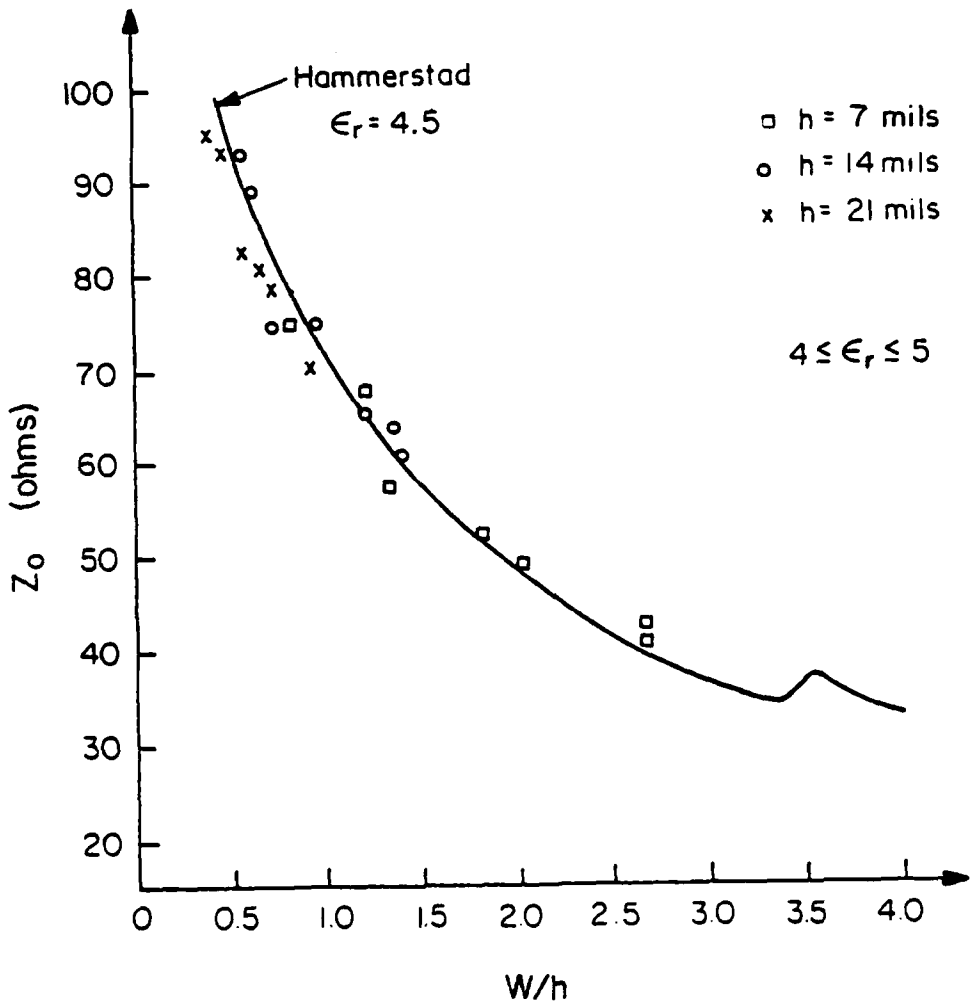

Figure 1.2 : Characteristic impedance Z_o versus width to height ; W/h. Solid line : theoretical expressions from Hammerstad with $\epsilon = 4.5$; points: experimental measurement using time domain reflectometry. For the experimental points, the lines have a dielectric constant $4 \leqslant \epsilon \leqslant 5$.

For $W/h \geq 2$,

$$\frac{W}{h} = \frac{2}{\pi}[B - 1 - \ln(2B - 1) + \frac{\epsilon_r - 1}{2\epsilon_r}(\ln(B - 1) + 0.39 - \frac{0.61}{\epsilon_r})] \tag{1.6}$$

where

$$A = \frac{Z_o}{60}\sqrt{\frac{\epsilon_r + 1}{2}} + \frac{\epsilon_r - 1}{\epsilon_r + 1}(0.23 - \frac{0.11}{\epsilon_r}) \tag{1.7}$$

and

$$B = \frac{377\pi}{2Z_o\sqrt{\epsilon_r}} \tag{1.8}$$

These relations assume an infinitely thin conductor strip ; in practice, the thickness must be considered, which is done by defining an effective width of the strip, W_e, for use with Equations (1.5) -(1.8) instead of W.

For $W/h \geq \frac{1}{2\pi}$,

$$W_e = \frac{W}{h} + \frac{t}{\pi h}(1 + 2\frac{h}{t}) \tag{1.9}$$

For $W/h \leq \frac{1}{2\pi}$,

$$\frac{W_e}{h} = W_h + \frac{t}{\pi h}[1 + \ln(\frac{4\pi W}{t})] \tag{1.10}$$

It has been found that for $t/h \leq 0.005$, $2 \leq \epsilon_r \leq 1$, and $0.1 \leq W/h \leq 0.5$, neglecting

the thickness of the strip introduced very little error. Since these values represent most practical cases, correction for finite thickness is often neglected.

1.3 Frequency Dependence and Dispersion

The relations derived above were based on the quasi-TEM model. At higher frequencies this model is not accurate for microstrip lines because of the propagation of hybrid modes. As the frequency increases, the phase velocity decreases which reveals an increase of the effective dielectric constant ; an increase of the characteristic impedance is also observed.

The frequency f_o below which dispersion effects can be ignored is given by [11]

$$f_o(Ghz) = 0.3\sqrt{\frac{Z_o}{h(cm)\sqrt{\epsilon_r} - 1}} \tag{1.11}$$

and the effective dielectric constant $\epsilon_e(f)$, is given by [12]

$$\epsilon_e = \epsilon_r - \frac{\epsilon_r - \epsilon_f}{1 + G(\frac{f}{f_p})^2} \tag{1.12a}$$

where

$$f_p = \frac{Z_o}{8\pi h} \tag{1.12b}$$

$$G = 0.6 + 0.009Z_o \tag{1.12c}$$

The frequency dependence of the characteristic impedance Z_o, was reported by Owens [13]

$$Z_o(f) = \frac{377h}{W_e(f)\sqrt{\epsilon_e(f)}} \tag{1.13}$$

where $W_e(f)$ is the effective width given by

$$W_e(f) = W + \frac{W_e(0) - W}{1 + (\frac{f}{f_p})} \tag{1.14}$$

$W_e(0)$ is obtained from (1.13) when f =0.

1.4 Time and Frequency Domain Characterization

The steady-state, single frequency solutions for the voltage and current on a transmission line derived from Maxwell's equations [14] have the form

$$V(t,x) = [A\, e^{-j\frac{\omega x}{v_p}} + B\, e^{+j\frac{\omega x}{v_p}}]\, e^{j\omega t} \tag{1.15}$$

$$I(t,x) = \frac{1}{Z_o}[A\, e^{-j\frac{\omega x}{v_p}} - B\, e^{+j\frac{\omega x}{v_p}}]\, e^{j\omega t} \tag{1.16}$$

where A and B are constants which depend on the terminations. This can be rewritten in a more general form which accounts for the transients in the line :

$$V(t,x) = V_+(t,x) + V_-(t,x) \tag{1.17}$$

$$I(t,x) = \frac{1}{Z_o}[V_+(t,x) - V_-(t,x)] \tag{1.18}$$

1.4.1 Time Domain

Experimental determination of microstrip line characteristics is classically performed using Time Domain Reflectometry (TDR) techniques. Reference [15] gives a complete overview of the basic principles and their uses for network transient measurement. To visualize the technique, let us consider the test set up shown in Fig. 1.3a : the system consists of a

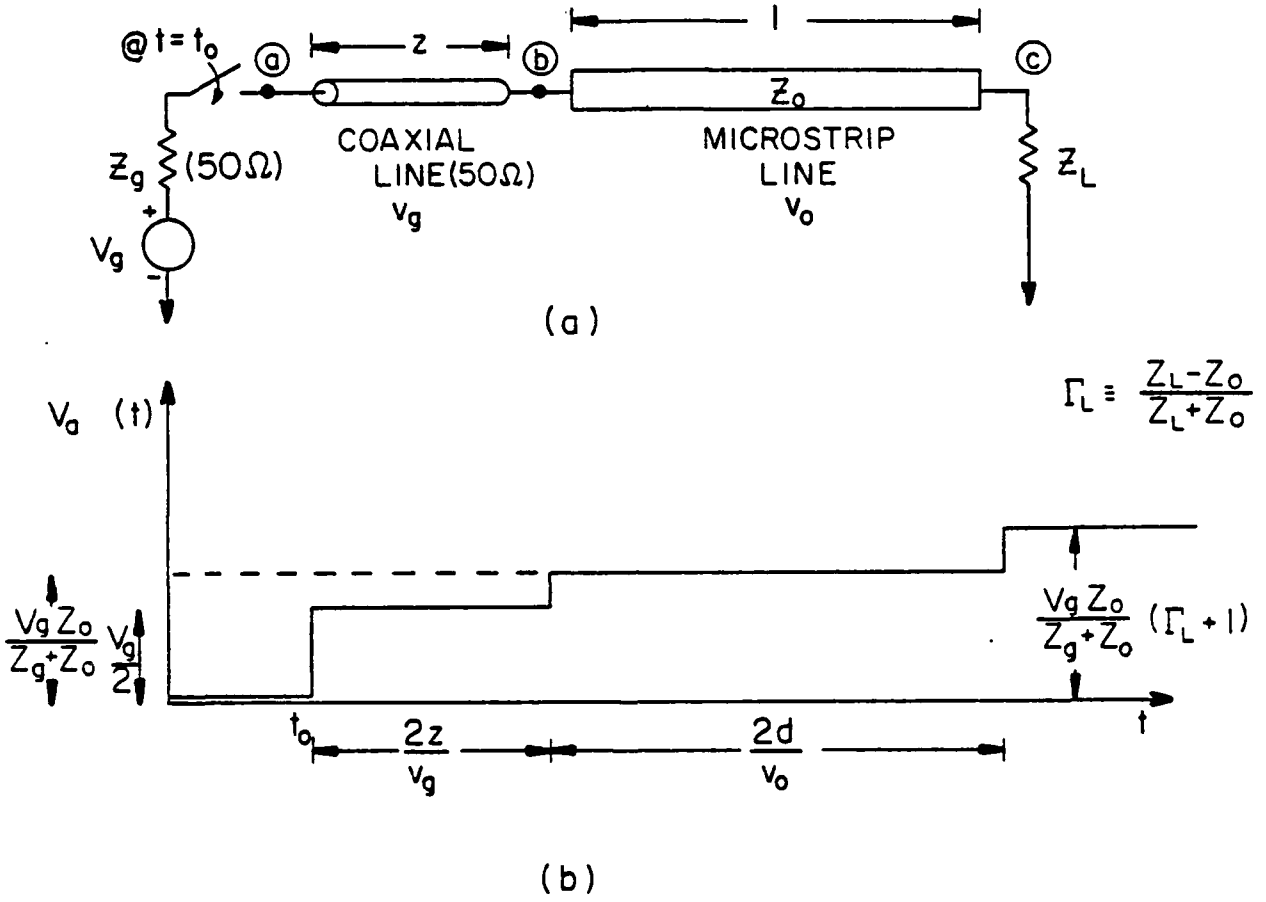

Figure 1.3 : Time Domain Reflectometry. Applications to transmission line characterization:(a) experimental setup , (b) voltage reading. The time axis can also be used as position axis which allows to determine and locate discontinuities along the test line. Rise time of applied step ≈ 50 *ps*.

ramp generator V_g of internal resistance Z_g (usually 50 Ω). A coaxial cable of characteristic impedance Z_g and length l is connected to the line to be tested (characteristic impedance Z_o and length l). When the switch is closed at $t = t_o$, a forward moving wave C_+ is generated at point a. For voltage and current continuity, it must satisfy

$$\frac{V_g - C_+}{Z_g} = \frac{C_+}{Z_g} \tag{1.19}$$

from which we obtain

$$C_+ = \frac{V_g}{2} \tag{1.20}$$

Upon reaching the test line at point b, a backward wave C_- as well as a forward wave T_+ appear. They must satisfy

$$C_+ + C_- = T_+ \tag{1.21a}$$

$$\frac{C_+ - C_-}{Z_g} = \frac{T_+}{Z_o} \tag{1.21b}$$

which yields

$$C_- = \left(\frac{Z_o - Z_g}{Z_o + Z_g}\right) C_+ = \Gamma_g C_+ \tag{1.22a}$$

$$T_+ = \frac{2Z_o C_+}{Z_o + Z_g} \tag{1.22b}$$

where Γ_g is the reflection coefficient from the test line at b. When T_+ reaches the end of the

test line at point c, a reflected wave T_- is produced such that

$$T_- = (\frac{Z_L - Z_o}{Z_L + Z_o})T_+ = \Gamma_L T_+ \tag{1.23}$$

where Γ_L is the reflection coefficient at the load. Upon reaching b, T_- will generate two new waves : C_- on the coaxial line and T'_+on the test line. These successive reflections will keep taking place indefinitely. The expression for the voltage at any point along the line will have the form of a geometric series of $\Gamma_g \Gamma_L$ which converges to the final value (for very large t)

$$V = \frac{Z_L}{Z_L + Z_g} V_g \tag{1.24}$$

Figure 1.3b shows a graph of the voltage at point a, $V_a(t)$ as a function of time. Since the phase velocity in both coaxial and test lines are assumed constant, there exist a linear relationship between time and position. The first step in the voltage is the magnitude of the forward wave traveling the coaxial cable C_+. Its duration is $2l/v_c$ where v_c is the velocity in the coaxial line. The second step is T_+. If the magnitudes are normalized to C_+, the difference between C_+ and T_+ is the reflection coefficient Γ_o due to the test line

$$\Gamma_o = \frac{Z_o - Z_g}{Z_o + Z_g} \tag{1.25}$$

When Γ_o is read from the Time Domain Reflectometer, it allows direct calculation of Z_o :

$$Z_o = Z_g(\frac{1 + \Gamma_o}{1 - \Gamma_o}) \tag{1.26}$$

Whereas the phase velocity v_o can be obtained from the time delay τ_o :

$$v_o = 2\frac{l}{\tau_o} \tag{1.27}$$

Capacitance and inductance per unit length can be extracted using (1.1)-(1.3).

$$C_s = \frac{1}{Z_o v_o} \tag{1.28a}$$

and

$$L_s = \frac{Z_o}{v_o} \tag{1.28b}$$

1.4.2 Frequency Domain - Scattering Parameter Model

The information obtained from the TDR, although complete, does not provide us with any insight of the frequency dependence of the transmission line parameters. Because of instability concerns at large frequencies (RF and microwave) and because of their manoeuvrability at those frequencies, Scattering parameters (S parameters) can be used for a frequency domain analysis. A good introduction to S parameters is given in References [16] and [17]. We briefly summarize the essentials of these parameters and their meanings.

Figure 1.4 shows a two-port network inserted on a line of characteristic impedance Z_o. Both ends of the line can be regarded as connected to generators of internal impedance Z_o. E_{i1} and E_{i2} are the incident portions of the voltages in ports 1 and 2, respectively. Similarly, E_{r1} and E_{r2} are the reflected portions of the same voltages. We can then define four traveling waves on the line :

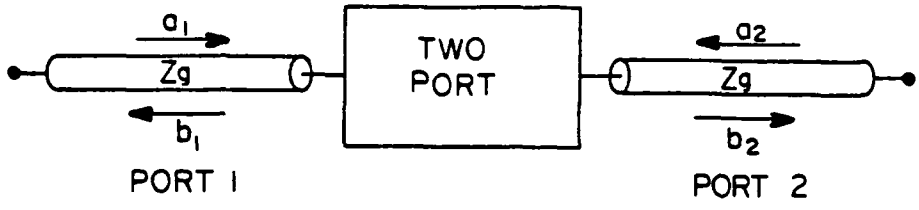

$$b_1 = S_{11}a_1 + S_{12}a_2$$
$$b_2 = S_{21}a_1 + S_{22}a_2$$

Figure 1.4 : Scattering matrix. Definition in terms of the power waves.

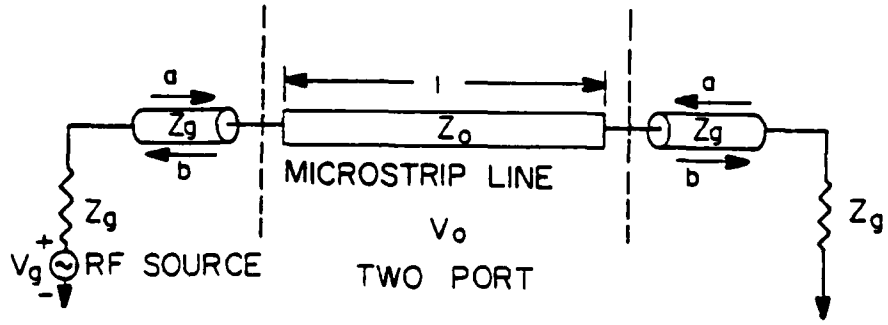

$$\Gamma = \frac{Z_o - Z_g}{Z_o + Z_g}$$

$$S_{11} = S_{22} = \frac{(1 - e^{-2j\frac{\omega l}{V_o}})\,\Gamma}{1 - \Gamma^2 e^{-2j\frac{\omega l}{V_o}}}$$

$$S_{12} = S_{21} = \frac{(1-\Gamma^2)\, e^{-j\frac{\omega l}{V_o}}}{1 - \Gamma^2 e^{-2j\frac{\omega l}{V_o}}}$$

Figure 1.5 : Experimental setup for determining the characteristic of a microstrip line as a function of frequency. Equations are shown that relate the velocity and the impedance to the measured reflection and transmission parameters.

$$a_1 = \frac{E_{i1}}{\sqrt{Z_o}} \qquad a_2 = \frac{E_{i2}}{\sqrt{Z_o}} \tag{1.29a}$$

$$b_1 = \frac{E_{r1}}{\sqrt{Z_o}} \qquad b_2 = \frac{E_{r2}}{\sqrt{Z_o}} \tag{1.29b}$$

The square of the magnitude of these new variables has the dimension of power ; $|a_1|^2$ is the incident power to port 1 ; $|b_2|^2$ is the reflected power from port 2 of the network. The four S parameters characterizing the two-port relate the traveling waves as follows :

$$b_1 = S_{11}a_1 + S_{12}a_2 \tag{1.30a}$$

$$b_2 = S_{21}a_1 + S_{22}a_2 \tag{1.30b}$$

From these relations, the four S parameters can be defined alternatively as

$$S_{11} = \frac{b_1}{a_1}\Big|_{a_2=0} \qquad S_{21} = \frac{b_2}{a_1}\Big|_{a_2=0} \tag{1.30c}$$

$$S_{12} = \frac{b_1}{a_2}\Big|_{a_1=0} \qquad S_{22} = \frac{b_2}{a_2}\Big|_{a_1=0} \tag{1.30d}$$

If both ends of the line are connected to generators with internal impedance Z_g, then a_1 and a_2 are simply the incident waves from the generators. Since the incident power from either generator can be deliberately set to zero, Equations (1.30c) and (1.30d) provide the main scheme for determining the S parameters of a network. It is of interest to note that S_{11} and S_{22} are reflection coefficients and relate traveling waves of one given port whereas S_{12} and S_{21} are the transmission coefficients of the two-port.

1.4.3 Scattering Matrix for Transmission Line

When the network to be characterized is a transmission line, it can be modeled as a two-port (Fig. 1.5). Consider an unknown transmission line of characteristic impedance Z_o and length l embedded between two coaxial lines of impedance Z_g terminated with their characteristic impedance. On the left is an RF source of frequency $f = \omega/2\pi$. Setting the origin at the first intersection , the voltage and current equations for the system are

$$V_1(x) = A\, e^{-j\frac{\omega x}{v_g}} + B\, e^{+j\frac{\omega x}{v_g}} \tag{1.31a}$$

$$I_1(x) = \frac{1}{Z_g}\left[A\, e^{-j\frac{\omega x}{v_g}} - B\, e^{+j\frac{\omega x}{v_g}}\right] \tag{1.31b}$$

$$V_2(x) = C\, e^{-j\frac{\omega x}{v_o}} + D\, e^{+j\frac{\omega x}{v_o}} \tag{1.32a}$$

$$I_2(x) = \frac{1}{Z_o}\left[C\, e^{-j\frac{\omega x}{v_o}} - D\, e^{+j\frac{\omega x}{v_o}}\right] \tag{1.32b}$$

v_g and v_o are the propagation velocities in the coaxial and test lines, respectively. A, B, C, and D are constants which depend on the terminations. Applying the boundary conditions at $x = 0$ and $x = l$, we obtain

$$S_{21} = \frac{V_2(l)}{A} = \frac{(1-\Gamma^2)\beta}{1-\Gamma^2\beta^2} \tag{1.33a}$$

$$S_{11} = \frac{B}{A} = \frac{(1-\beta^2)\Gamma}{1-\Gamma^2\beta^2} \tag{1.33b}$$

where

$$\beta = e^{-j\frac{\omega l}{v_p}} \tag{1.34a}$$

and

$$\Gamma = \frac{Z_o - Z_g}{Z_o + Z_g} \tag{1.34b}$$

Γ is the reflection coefficient at the ends of the unknown line. Adding (1.33) to (1.34), we get

$$S_{21} - S_{11} = \frac{\Gamma + \beta}{1 + \Gamma\beta} \tag{1.35}$$

Subtracting (1.34) from (1.33) gives

$$S_{21} - S_{11} = \frac{\Gamma - \beta}{1 - \Gamma\beta} \tag{1.36}$$

Combining (1.35) and (1.36) yields

$$\Gamma = \frac{S_{21}^2 - S_{11}^2 \pm \sqrt{1 + (S_{21}^2 - S_{11}^2) - 2(S_{21}^2 + S_{11}^2)}}{2S_{11}} \tag{1.37a}$$

$$\beta = \frac{S_{11}^2 - S_{21}^2 \pm \sqrt{1 + (S_{11}^2 - S_{21}^2) - 2(S_{11}^2 + S_{21}^2)}}{2S_{21}} \tag{1.37b}$$

Since S_{11} and S_{21} can be measured with a network analyzer, Equation (1.37) allows a direct determination of Γ from which Z_o can be obtained. The propagation velocity and the effective dielectric constant can also be obtained. Figure 1.6 shows experimental plots of characteristic impedance versus frequency for various geometries of lines. The measurements were performed on an HP 8505 automated network analyzer. At higher frequencies,

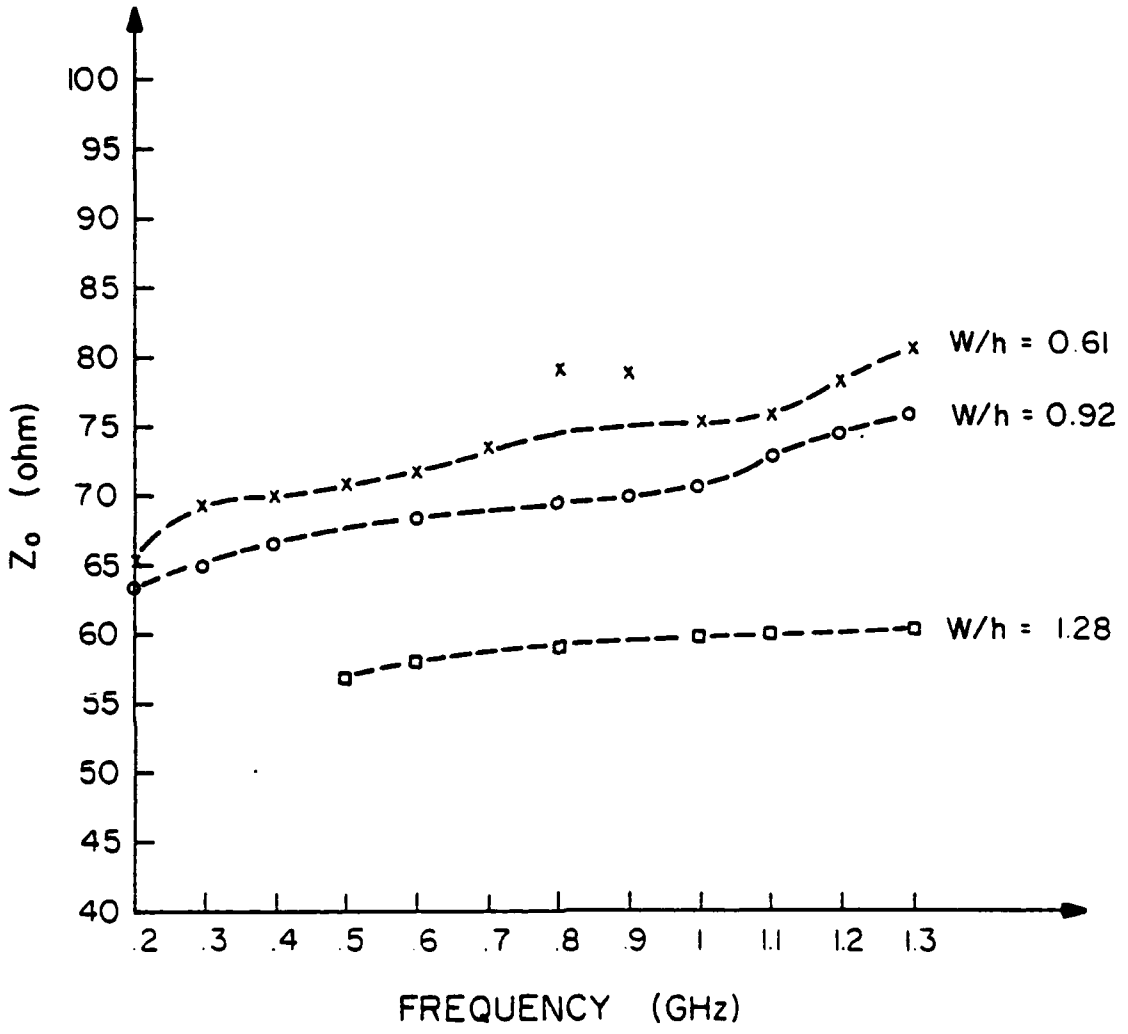

Figure 1.6 : Experimental plot of the characteristic impedance Z_o as a function of frequency for different geometries. The dashed lines are the best fit curves. Measurements were performed on an HP 8505 RF network analyzer and Equation (1.37) allowed determination of Z_o.

the measurements become more difficult and external effects such as junction discontinuities, capacitance, and inductance become more significant.

CHAPTER 2

COUPLED TRANSMISSION LINE CHARACTERISTICS

The theory of coupled transmission lines arose with the early applications to multiconductor systems. Its development continued with the advent of directional electromagnetic couplers [18]. Several methods using the quasi-TEM approximation have been proposed to obtain the parameters of coupled microstrip lines. A comparison of these methods is given in [19]. Krage and Haddad [20], [21] have determined the inductive and capacitive coupling coefficients as well as the directivity for various geometries of coupled lines. Bryant and Weiss [22] have established the relationship between the electrical and physical parameters of coupled line pairs using the Green's function approach. Their MSTRIP computer program has been validated after comparison with various authors. Garg and Bahl [23] derived semi-empirical equations for the even and odd mode parameters. Hammerstad and Jensen [24] succeeded in implementing a model with errors less than those caused by physical tolerance. Recently, Kirshing and Jensen [25] reported frequency dependent expressions with unprecedented accuracy. Most of the solutions provided by these numerical techniques suffer from the lack of experimental data which would validate their application to microstrip coupler design. The main difficulty arises with the presence of different modes of propagation and the parameters associated with these modes which impose more complex measurement technique requirements. The goal of this chapter consists of implementing the electrical model for coupled lines and determining experimentally the coupling parameters. Correlations between physical dimensions and electrical parameters can then be established empirically. Altough this method limits the flexibility of the microstrip designer, it provides more accuracy for parameter determination while giving a better insight of the coupling phenomena.

2.1 General Expressions and Propagation Modes

The differential equations relating the propagating voltage and current along two coupled transmission lines are

$$-\frac{\partial V_1}{\partial x} = L_{11}\frac{\partial I_1}{\partial t} + L_{12}\frac{\partial I_2}{\partial t} \tag{2.1a}$$

$$-\frac{\partial V_2}{\partial x} = L_{21}\frac{\partial I_1}{\partial t} + L_{22}\frac{\partial I_2}{\partial t} \tag{2.1b}$$

$$-\frac{\partial I_1}{\partial x} = C_{11}\frac{\partial V_1}{\partial t} + C_{12}\frac{\partial V_2}{\partial t} \tag{2.2a}$$

$$-\frac{\partial I_2}{\partial x} = C_{21}\frac{\partial V_1}{\partial t} + C_{22}\frac{\partial V_2}{\partial t} \tag{2.2b}$$

V_1 and V_2 are the voltages along line 1 and line 2, respectively, and I_1 and I_2 are the corresponding currents. The L_{ij} and C_{ij} are the matrix inductance and capacitance coefficients. The mutual terms are equivalent, C_{12}=C_{21} and L_{12}=L_{21}. Moreover for symmetric structures we also have L_{11}=L_{22} and C_{11}=C_{22}. Those matrix elements can be related to the electrical parameters. Figure 2.1b is the distributed model for two coupled identical lines for which C_s and L_s are the self-inductance and self-capacitance, respectively, and L_m and C_m, the mutual inductance and capacitance. Kirchhoff's law in differential form gives

$$-\frac{\partial V_1}{\partial x} = L_s\frac{\partial I_1}{\partial t} + L_m\frac{\partial I_2}{\partial t} \tag{2.3a}$$

$$-\frac{\partial V_2}{\partial x} = L_m\frac{\partial I_1}{\partial t} + L_s\frac{\partial I_2}{\partial t} \tag{2.3b}$$

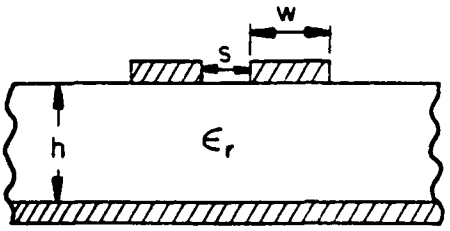

(a) COUPLED MICROSTRIP PAIR

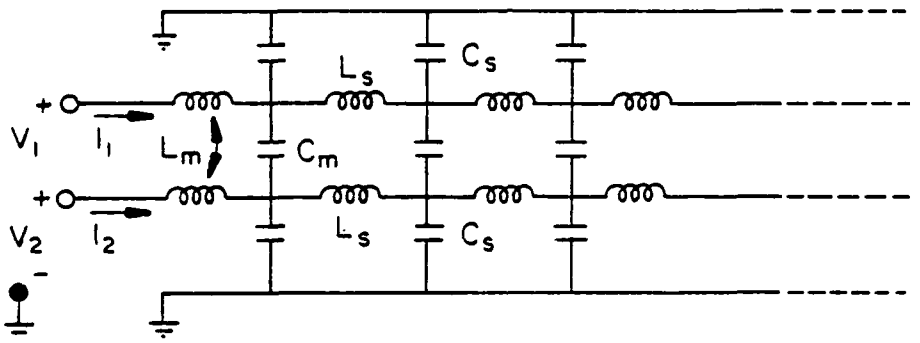

(b) CIRCUIT MODEL

Figure 2.1 : Coupled microstrip lines : (a) geometry, (b) distributed circuit equivalent. It is assumed that the two lines are identical. L_s and C_s are the self-inductance and capacitance of each line. L_m and C_m are the mutual parameters of the pair. These parameters can be measured and related to the matrix elements using Equations (2.5)-(2.8).

$$-\frac{\partial I_1}{\partial x} = C_s \frac{\partial V_1}{\partial t} + C_m \frac{\partial V_2}{\partial t} \tag{2.4a}$$

$$-\frac{\partial I_2}{\partial x} = C_m \frac{\partial V_1}{\partial t} + C_s \frac{\partial V_2}{\partial t} \tag{2.4b}$$

Comparison with Equations (2.1)-(2.2) with (2.3)-(2.4) gives the equivalences.

$$C_{11} = C_s + C_m \tag{2.5}$$

$$C_{12} = -C_m \tag{2.6}$$

$$L_{11} = L_s \tag{2.7}$$

$$L_{12} = L_m \tag{2.8}$$

For the symmetrical case one solution can be found by adding (2.1a) to (2.1b) and (2.2a) to (2.2b).

$$-\frac{\partial V_e}{\partial x} = (L_{11} + L_{12})\frac{\partial I_e}{\partial t} \tag{2.9a}$$

$$-\frac{\partial I_e}{\partial x} = (C_{11} + C_{12})\frac{\partial V_e}{\partial t} \tag{2.9b}$$

where

$$V_e = \frac{1}{2}(V_1 + V_2) \tag{2.10a}$$

$$I_e = \frac{1}{2}(I_1 + I_2) \tag{2.10b}$$

are the common mode voltage and current. Equations (2.9a) and (2.9b) have the same form as the well-known single line Telegraph Equations ; therefore the solutions in the frequency domain assuming a time harmonic dependence are

$$V_e(x) = A_e\, e^{-j\frac{\omega x}{v_e}} + B_e\, e^{+j\frac{\omega x}{v_e}} \tag{2.11a}$$

$$I_e(x) = \frac{A_e}{Z_e}\, e^{-j\frac{\omega x}{v_e}} - \frac{B_e}{Z_e}\, e^{+j\frac{\omega x}{v_e}} \tag{2.11b}$$

where A_e and B_e are constant coefficients associated with the forward and backward traveling waves, respectively. Z_e and v_e are the even mode impedance and propagation velocity, respectively :

$$Z_e = \sqrt{\frac{L_{11}+L_{12}}{C_{11}+C_{12}}} = \sqrt{\frac{L_s+L_m}{C_s}} \tag{2.12}$$

$$v_e = \frac{1}{\sqrt{(L_{11}+L_{12})(C_{11}+C_{12})}} = \frac{1}{\sqrt{(L_s+L_m)C_s}} \tag{2.13}$$

and $\omega=2\pi f$ is the angular frequency of the propagating signal. Subtracting (2.1b) from (2.1a) gives

$$-\frac{\partial V_d}{\partial x} = (L_{11}-L_{12})\frac{\partial I_d}{\partial t} \tag{2.14a}$$

$$-\frac{\partial I_d}{\partial x} = (C_{11}-C_{12})\frac{\partial V_d}{\partial t} \tag{2.14b}$$

where

$$V_d = \frac{1}{2}(V_1 - V_2) \tag{2.15a}$$

$$I_d = \frac{1}{2}(V_1 - V_2) \tag{2.15b}$$

are the differential mode voltage and current. As before this system can be solved to give

$$V_d(x) = A_d\, e^{-j\frac{\omega x}{v_d}} + B_d\, e^{+j\frac{\omega x}{v_d}} \tag{2.16a}$$

$$I_d(x) = \frac{A_d}{Z_d}\, e^{-j\frac{\omega x}{v_d}} - \frac{B_d}{Z_d}\, e^{+j\frac{\omega x}{v_d}} \tag{2.16b}$$

A_d and B_d are as before constant coefficients associated with the forward and backward waves, respectively, and Z_d and v_d are the odd mode impedance and propagation velocity defined as

$$Z_d = \sqrt{\frac{L_{11}-L_{12}}{C_{11}-C_{12}}} = \sqrt{\frac{L_s - L_m}{C_s + 2C_m}} \tag{2.17}$$

$$v_d = \frac{1}{\sqrt{(L_{11}-L_{12})(C_{11}-C_{12})}} = \frac{1}{\sqrt{(L_s - L_m)(C_s + 2C_m)}} \tag{2.18}$$

Using Equations (2.10) and (2.15) we obtain the general solution for the line currents and voltages :

$$V_1(x) = V_e(x) + V_d(x) \tag{2.19a}$$

$$I_1(x) = I_e(x) + I_d(x) \tag{2.19b}$$

$$V_2(x) = V_e(x) - V_d(x) \tag{2.20a}$$

$$I_2(x) = I_e(x) - I_d(x) \tag{2.20b}$$

which gives

$$V_1(x) = A_e\, e^{-j\frac{\omega x}{v_e}} + B_e\, e^{+j\frac{\omega x}{v_e}} + A_d\, e^{-j\frac{\omega x}{v_d}} + B_d\, e^{+j\frac{\omega x}{v_d}} \tag{2.21a}$$

$$I_1(x) = \frac{A_e}{Z_e} e^{-j\frac{\omega x}{v_e}} - \frac{B_e}{Z_e} e^{+j\frac{\omega x}{v_e}} + \frac{A_d}{Z_d} e^{-j\frac{\omega x}{v_d}} - \frac{B_d}{Z_d} e^{+j\frac{\omega x}{v_d}} \tag{2.21b}$$

$$V_2(x) = A_e\, e^{-j\frac{\omega x}{v_e}} + B_e\, e^{+j\frac{\omega x}{v_e}} - A_d\, e^{-j\frac{\omega x}{v_d}} - B_d\, e^{+j\frac{\omega x}{v_d}} \tag{2.22a}$$

$$I_2(x) = \frac{A_e}{Z_e} e^{-j\frac{\omega x}{v_e}} - \frac{B_e}{Z_e} e^{+j\frac{\omega x}{v_e}} - \frac{A_d}{Z_d} e^{-j\frac{\omega x}{v_d}} + \frac{B_d}{Z_d} e^{+j\frac{\omega x}{v_d}} \tag{2.22b}$$

Equations (2.21) and (2.22) give the general form for the line currents and voltages for a time harmonic excitation. The constants A_e, B_e, A_d, and B_d are determined by the boundary conditions at the four ends of the lines. Determination of these constants depends on the nature of the problem. For the case where the excitation is periodic, a Fourier series form must be assumed as the general solution for which the constants become the Fourier series coefficients. Finally for nonperiodic excitation, a Fourier transform approach must be used for the general solution. This will be illustrated in the next chapter. In all cases, the time-dependent solutions have the form :

$$V_1(x) = a_e(t - \frac{x}{v_e}) + b_d(t + \frac{x}{v_e}) + a_d(t - \frac{x}{v_d}) + b_d(t + \frac{x}{v_d}) \tag{2.23a}$$

$$I_1(x) = \frac{1}{Z_e}[a_e(t - \frac{x}{v_e}) - b_e(t + \frac{x}{v_e})] + \frac{1}{Z_d}[a_d(t - \frac{x}{v_d}) - b_d(t + \frac{x}{v_d})] \qquad (2.23b)$$

$$V_2(x) = a_e(t - \frac{x}{v_e}) + b_e(t + \frac{x}{v_e}) - a_d(t - \frac{x}{v_d}) - b_d(t + \frac{x}{v_d}) \qquad (2.24a)$$

$$I_2(x) = \frac{1}{Z_e}[a_e(t - \frac{x}{v_e}) - b_e(t + \frac{x}{v_e})] - \frac{1}{Z_d}[a_d(t - \frac{x}{v_d}) - b_d(t + \frac{x}{v_d})] \qquad (2.24b)$$

a_e and a_d are the forward functions for the even and odd modes, respectively, b_e and b_d are the backward functions for the same modes.

2.2 Application and Coupling Parameter Measurement

The major advantage of Equations (2.23) and (2.24) is that the solutions are put in a form where the reflected waves are separated in time from the forward waves. This can be applied with TDR measurements to obtain the coupling parameters of a microstrip pair since only the forward voltage waves need to be considered. In Figure 2.2a, two identical coupled lines of length l are connected at x = 0. A coaxial cable of characteristic impedance Z_g connects the TDR to the pair. A forward traveling voltage step of magnitude V_f upon reaching the junction generates a backward step, V_b. From Kirchhoff's law we must have

$$V_{td} = a_e(t,0) + a_d(t,0) = V_f + V_b \qquad (2.25a)$$

$$I_{td} = \left| a_e \frac{(t,0)}{Z_e} + a_d \frac{(t,0)}{Z_d} \right| + \left| a_e \frac{(t,0)}{Z_e} - a_d \frac{(t,0)}{Z_d} \right| = \frac{V_f - V_b}{Z_g} \qquad (2.25b)$$

$$V_{td} = a_e(t,0) - a_d(t,0) \qquad (2.26)$$

This implies that

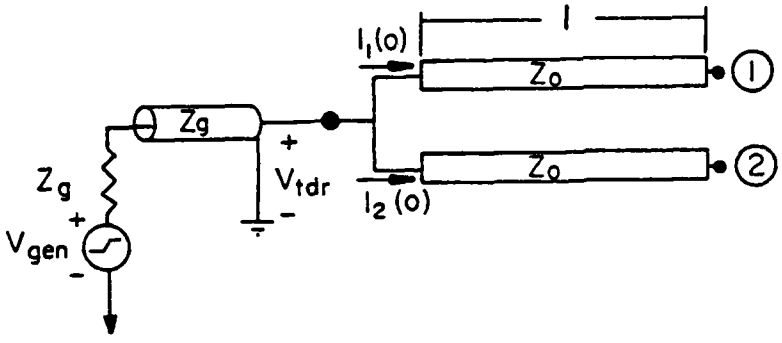

$$Ze = 2\left(\frac{1+\rho_e}{1-\rho_e}\right) Z_g$$

$$Ve = \frac{2l}{\text{time delay}}$$

(NO ODD MODE)

(a) EVEN MODE IMPEDANCE DETERMINATION

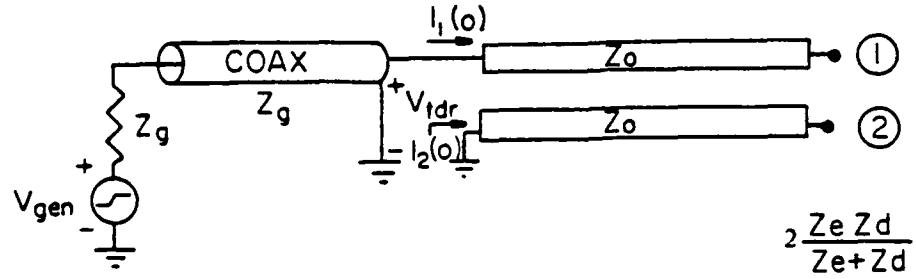

$$2\frac{Ze\,Zd}{Ze+Zd} = \left(\frac{1+\rho_p}{1-\rho_p}\right) Z_g$$

(b) "PARALLEL" CONNECTION

Figure 2.2 : Experimental determination of the even and odd mode characteristics of a pair of coupled transmission lines : (a) even mode measurement since no odd mode is present both velocity and impedance for this mode can be measured ; (b) parallel connection since it is difficult to excite the odd mode, this configuration is used to determine the parallel combination of Z_{even} and Z_{odd}.

$$a_d(t,0) = 0 \tag{2.27}$$

and

$$\frac{V_{tdr}}{I_{tdr}} = \frac{Z_e}{2} \tag{2.28}$$

Therefore, the reflection coefficient measured at $x=0$, $\rho_e = V_b/V_f$ can be related to the even mode impedance of the pair :

$$Z_e = 2\left(\frac{1+\rho_e}{1-\rho_e}\right)Z_g \tag{2.29}$$

Since no odd mode exists, the measured time delay τ_e, can be related to the even mode velocity :

$$v_e = 2\frac{l}{\tau_e} \tag{2.30}$$

Another configuration is that of Figure 2.2b in which line 2 is connected to ground at x = 0 and line 1 is connected to the coaxial line. The equations are

$$V_{tdr} = a_e(t,0) + a_d(t,0) = V_f + V_b \tag{2.31a}$$

$$I_{tdr} = \left| a_e\frac{(t,0)}{Z_e} + a_d\frac{(t,0)}{Z_d} \right| = \frac{V_f - V_b}{Z_g} \tag{2.31b}$$

$$a_e(t,0) = a_d(t,0) \tag{2.32a}$$

$$\frac{V_{td}}{I_{td}} = 2\frac{Z_e Z_d}{Z_e + Z_d} \tag{2.32b}$$

The associated reflection coefficient $\rho_p = V_b/V_f$ can be measured directly and using the above relations we obtain

$$\frac{Z_e Z_d}{Z_e + Z_d} = Z_g\left(\frac{1+\rho_p}{1-\rho_p}\right) \tag{2.33}$$

Since both even and odd modes are propagating , a direct relation between the time delay and either velocity cannot be established. Nevertheless, Equations (2.29), (2.30), and (2.33) provide the necessary relationship for extracting Z_e, Z_d, v_e and, if the single line parameters are known, Equations (2.12), (2.13), (2.17), and (2.18) can be used to determine the mutual capacitance and inductance as well as the odd mode propagation velocity of the pair (Figure 2.3). From these equations we see that

$$Z_d < Z_o < Z_e \tag{2.34}$$

which suggests that for weak coupling

$$Z_d \approx Z_o \approx Z_e \tag{2.35}$$

Table 1 shows experimental values of self and coupling parameters obtained for several microstrip pairs. These values were extracted by using the methods outlined above. As expected mutual parameters depend strongly on the spacing between the lines ; it is also observed that the mutual inductance is stronger even at wider spacings between the edges of the coupled lines.

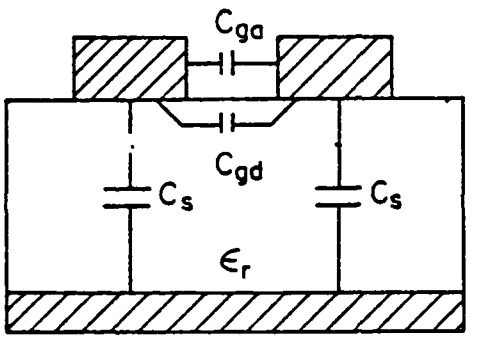

C_s : SELF-CAPACITANCE
C_m : MUTUAL CAPACITANCE
L_s : SELF-INDUCTANCE
L_m : MUTUAL INDUCTANCE

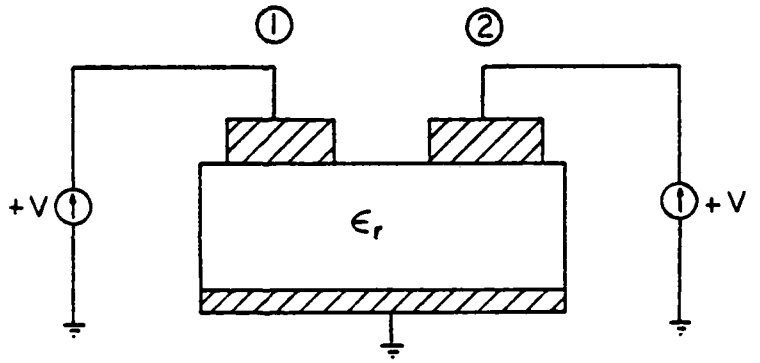

EVEN MODE: $V_1 = V_2$

$$Z_e = \sqrt{\frac{L_s + L_m}{C_s}}$$

$$v_e = \frac{1}{\sqrt{C_s(L_s+L_m)}}$$

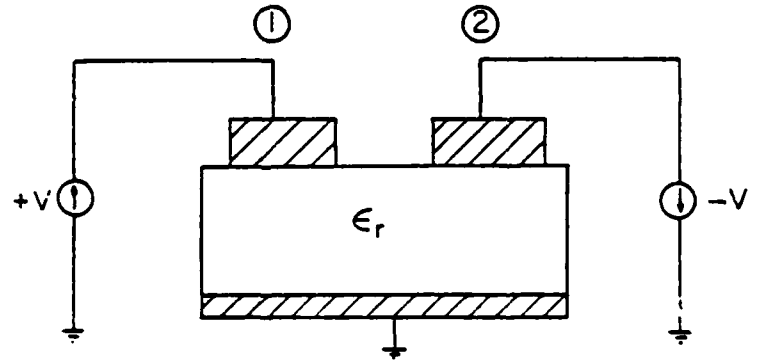

ODD MODE: $V_1 = V_2$

$$Z_o = \sqrt{\frac{L_s - L_m}{C_s + 2C_m}}$$

$$v_o = \frac{1}{\sqrt{(L_s-L_m)(C_s+2C_m)}}$$

Figure 2.3 : Diagram showing the configurations for exciting even and odd modes and relations between characteristic impedance, propagation velocity, and the self- and coupling parameters of the pair.

TABLE 1 : EXPERIMENTAL DATA OBTAINED FOR VARIOUS GEOMETRIES OF TRANSMISSION LINES WITH GLASS-EPOXY DIELECTRIC. GEOMETRICAL DIMENSIONS ARE AS DEFINED IN FIGURE 2.1, THEIR UNIT IS IN MILS. IMPEDANCES ARE IN OHMS AND VELOCITIES ARE IN m / ns. INDUCTANCES AND CAPACITANCES ARE IN nH/m AND pF/m, RESPECTIVELY.

Design Width = 10 mils Dielectric height :21 mils

S	Zo	Vo	Zd	Vd	Ze	Ve	Ls	Cs	Lm	Cm
5	93	.187	45	.162	127	.156	496	58	219.7	40
7	93	.187	51	.167	122	.159	496	58	191.3	30
10	93	.187	54	.177	123	.159	496	58	171.3	23
12	93	.187	58	.182	120	.161	496	58	157.5	19
14	93	.187	60	.167	113	.166	496	58	150.1	21
16	93	.187	62	.162	108	.169	496	58	113.2	21
18	93	.187	64	.157	104	.172	496	58	39.2	21
20	93	.187	65	.156	102	.174	496	58	77.6	20

Design Width = 15 mils Dielectric height :21 mils

S	Zo	Vo	Zd	Vd	Ze	Ve	Ls	Cs	Lm	Cm
3	78	.182	39	.192	116	.148	429	70	224.8	31
5	78	.182	44	.198	113	.150	429	70	205.4	22
7	78	.182	47	.200	111	.151	429	70	192.8	18
10	78	.182	52	.206	107	.154	429	70	174.4	11
12	78	.182	58	.212	104	.156	429	70	156.5	6
14	78	.182	59	.207	102	.158	429	70	144.9	6
16	78	.182	60	.203	100	.159	429	70	133.6	6
18	78	.182	61	.198	98	.161	429	70	122.4	6
20	78	.182	62	.190	94	.164	429	70	100.8	7

Design Width = 20 mils Dielectric height :21 mils

S	Zo	Vo	Zd	Vd	Ze	Ve	Ls	Cs	Lm	Cm
3	72	.182	37	.161	99	.154	395	76	162.3	45
5	72	.182	42	.176	98	.154	395	76	156.7	30
7	72	.182	45	.174	94	.157	395	76	135.1	25
10	72	.182	52	.200	92	.157	395	76	135.5	10
12	72	.182	54	.205	90	.158	395	76	129.4	7
14	72	.182	57	.206	88	.160	395	76	119.0	4
16	72	.182	58	.202	86	.161	395	76	108.8	5
18	72	.182	59	.204	85	.162	395	76	104.1	3
20	72	.182	60	.194	82	.165	395	76	86.3	5

Since different charge distributions arise with the two modes, some authors have found it convenient to define an even mode capacitance and C_{ev} and an odd mode capaciance C_{od} and base the complete analysis in terms of these parameters [8], [9]. Figure 2.4 shows a decomposition of the total capacitance of a microstrip pair in terms of even and odd mode capacitances. The existing expressions for C_{ev} and C_{od} are semi-empirical, however, using our model, it can be shown that $C_{ev} = C_s$ and $C_{od} = C_s + 2C_m$.

The major advantage of the techniques of measurement introduced above is that they are very accurate, since no approximation was made in deriving the model and the relations between the coupling and propagation parameters. As a consequence, reliable empirical data can be established from these measurements and used as design guidelines for microstrip couplers.

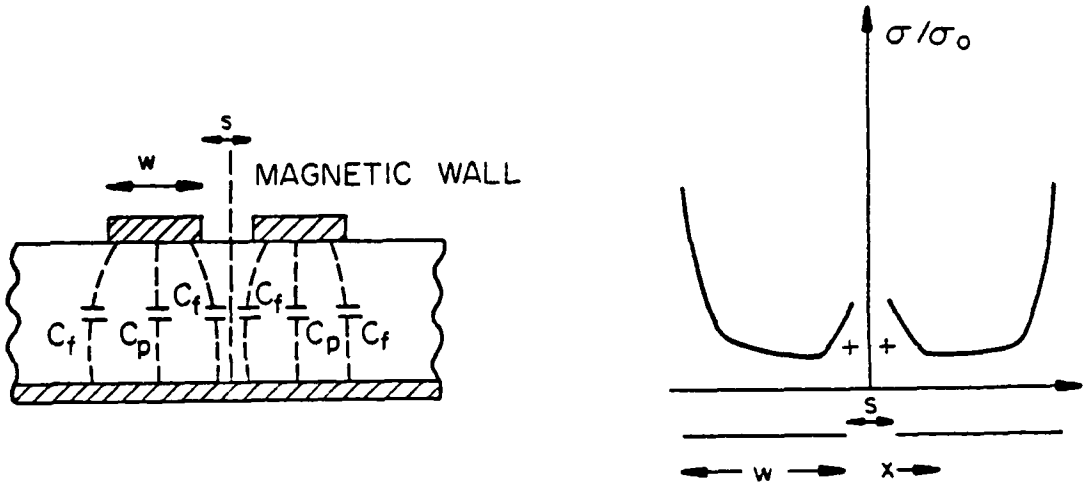

(a) EVEN MODE

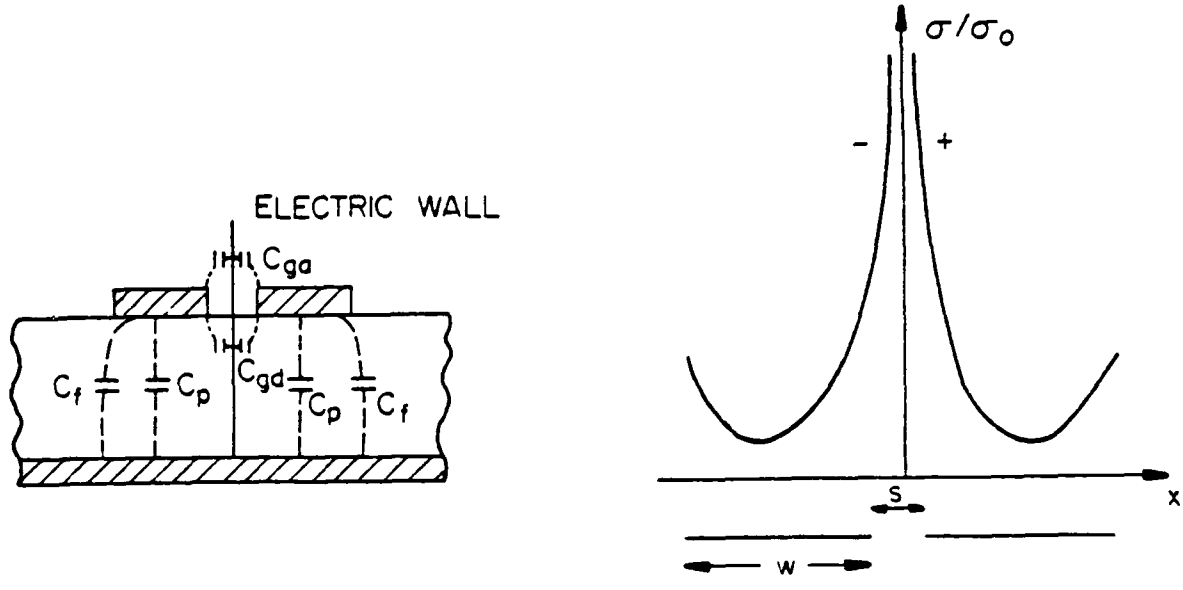

(b) ODD MODE

Figure 2.4 : Decomposition of the capacitances into odd and even mode components. C_p represents the capacitance associated with the TEM propagation mode ; C_f is the fringing capacitance. C_{ga} and C_{gd} are the mutual capacitances in air and in the dielectric, respectively. The normalized charge distribution associated with each mode is shown on the right with σ_0 being the charge at the center of each strip.

CHAPTER 3

TRANSIENTS IN COUPLED MICROSTRIP LINES

In the preceding chapter, the response of coupled lines was analyzed for harmonic (single frequency) excitation. We now wish to extend the analysis to account for the transients involved in the case of an arbitrary excitation. This is particularly important for digital applications where the signal applied to microstrip lines is a pulse or an impulse. Since the rise and fall times of these excitations are becoming shorter, the coupling between adjacent lines becomes more significant and has more serious effects. This is the so-called "crosstalk" noise. Various authors have attempted to describe this coupling phenomenon and relate it to the mutual parameters of the pair. Cotte [26] developed a first theory on the propagation of pulses in a coupled pair of conductors. Catt [27] analyzed the same effects for various transmission line configurations. Jarvis [28] studied the waveform distortion caused by this coupling as well as the effects of the terminations. Several numerical techniques have also been applied for simulation of these coupling effects. In general, the cross-coupling between two lines is a function of the terminations which make up the boundary conditions for the general solution previously derived. This chapter will examine the solution to this problem in the time domain.

3.1 Passive Terminations

Many practical situations in digital applications involve pairs of microstrip lines for which the the behavior of the terminations does not vary with the magnitude of the signals. In this case a real linear impedance can be used to model the terminations at the source and at the load. Figure 3.1 shows a microstrip pair having resistances Z_{s1} and Z_{s2} at the sending end and Z_{L1} and Z_{L2} at the far end. The voltage sources have magnitudes V_{s1} and V_{s2}. The time harmonic solution for the voltages and currents was found to be

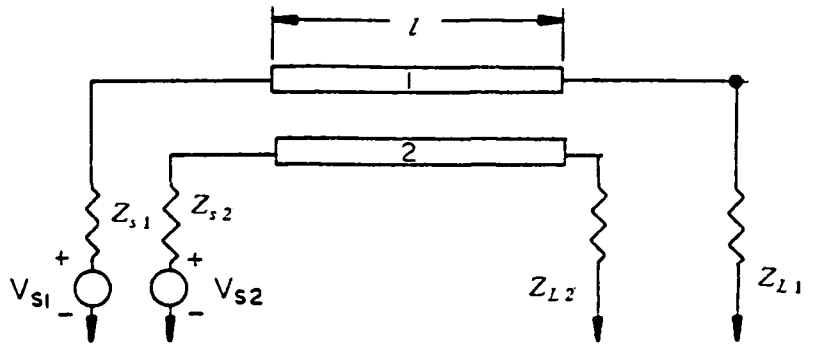

(a)

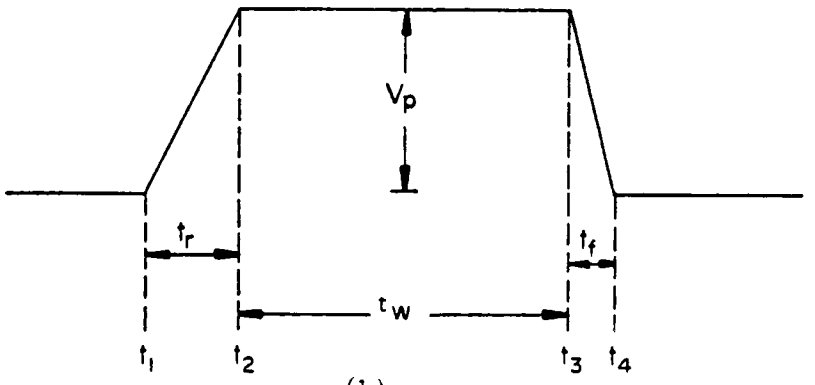

(b)

Figure 3.1 : (a) Representation of a microstrip pair loaded with passive terminations. The lines are assumed to be identical. V_{s1} and V_{s2} are arbitrary voltage sources. (b) Representation of a source waveform in the case of pulse excitation.

$$V_1(x) = A_e\, e^{-j\frac{\omega x}{v_e}} + B_e\, e^{+j\frac{\omega x}{v_e}} + A_d\, e^{-j\frac{\omega x}{v_d}} + B_d\, e^{+j\frac{\omega x}{v_d}} \tag{3.1a}$$

$$I_1(x) = \frac{A_e}{Z_e} e^{-j\frac{\omega x}{v_e}} - \frac{B_e}{Z_e} e^{+j\frac{\omega x}{v_e}} + \frac{A_d}{Z_d} e^{-j\frac{\omega x}{v_d}} - \frac{B_d}{Z_d} e^{+j\frac{\omega x}{v_d}} \tag{3.1b}$$

$$V_2(x) = A_e\, e^{-j\frac{\omega x}{v_e}} + B_e\, e^{+j\frac{\omega x}{v_e}} - A_d\, e^{-j\frac{\omega x}{v_d}} - B_d\, e^{+j\frac{\omega x}{v_d}} \tag{3.2a}$$

$$I_2(x) = \frac{A_e}{Z_e} e^{-j\frac{\omega x}{v_e}} - \frac{B_e}{Z_e} e^{+j\frac{\omega x}{v_e}} - \frac{A_d}{Z_d} e^{-j\frac{\omega x}{v_d}} + \frac{B_d}{Z_d} e^{+j\frac{\omega x}{v_d}} \tag{3.2b}$$

If we apply the boundary conditions at $x = 0$ and at $x = l$, namely

$$V_{s1} = V_2(0) + Z_{s1} I_1(0) \tag{3.3a}$$

$$V_{s2} = V_2(0) + Z_{s2} I_2(0) \tag{3.3b}$$

$$0 = V_1(l) - Z_{L1} I_1(l) \tag{3.3c}$$

$$0 = V_2(l) - Z_{L2} I_2(l) \tag{3.3d}$$

and by setting

$$m = \frac{Z_{s1}}{Z_e} \quad v = \frac{Z_{s2}}{Z_e} \quad q = \frac{Z_{L1}}{Z_e} \quad d = \frac{Z_{L2}}{Z_e} \tag{3.4a}$$

$$s = \frac{Z_{s1}}{Z_d} \quad y = \frac{Z_{s2}}{Z_d} \quad z = \frac{Z_{L1}}{Z_d} \quad p = \frac{Z_{L2}}{Z_d} \tag{3.4b}$$

$$\theta_{\cdot} = e^{-j\frac{\omega l}{v_{\cdot}}} \quad \alpha_{\cdot} = e^{+j\frac{\omega l}{v_{\cdot}}} \tag{3.4c}$$

$$\theta_d = e^{-j\frac{\omega l}{v_d}} \qquad \alpha_d = e^{+j\frac{\omega d}{v_d}} \tag{3.4d}$$

we arrive at

$$\begin{bmatrix} (1+m) & (1-m) & (1+s) & (1-s) \\ (1+v) & (1-v) & -(1+y) & (y-1) \\ \theta_e(1-q) & \alpha_e(1+q) & \theta_d(1-z) & \alpha_d(1+z) \\ \theta_e(1-d) & \alpha_e(1+d) & \theta_d(p-1) & -\alpha_d(1+p) \end{bmatrix} \begin{bmatrix} A_e \\ B_e \\ A_d \\ B_d \end{bmatrix} = \begin{bmatrix} V_{s1} \\ V_{s2} \\ 0 \\ 0 \end{bmatrix} \tag{3.5}$$

which is the generalized matrix equation for the coefficients A_e, B_e, A_d, and B_d.

In many practical cases, the terminations on both lines are identical, or $Z_{s1}=Z_{s2}=Z_s$ and $Z_{L1}=Z_{L2}=Z_L$. This reduces Equation (3.5) to a much simpler form. Then Cramer's Determinant Rule can be applied to give

$$A_e = \frac{(V_{s1}+V_{s2})Z_e}{2(Z_e+Z_s)} \quad \frac{1}{1-\Gamma_{se}\Gamma_{Le}\theta_e^2} \tag{3.6a}$$

$$B_e = \frac{-(V_{s1}+V_{s2})Z_e\theta_e^2\Gamma_{Le}^2}{2(Z_e+Z_s)} \quad \frac{1}{1-\Gamma_{se}\Gamma_{Le}\theta_e^2} \tag{3.6b}$$

$$A_d = \frac{(V_{s1}-V_{s2})Z_d}{2(Z_d+Z_s)} \quad \frac{1}{1-\Gamma_{sd}\Gamma_{Ld}\theta_d^2} \tag{3.7a}$$

$$B_d = \frac{-(V_{s1}-V_{s2})Z_d\theta_d^2\Gamma_{Ld}^2}{Z_d+Z_s} \quad \frac{1}{1-\Gamma_{sd}\Gamma_{Ld}\theta_d^2} \tag{3.7b}$$

where

$$\Gamma_{se} = \frac{Z_s-Z_e}{Z_s+Z_e} \qquad \Gamma_{Le} = \frac{Z_L-Z_e}{Z_L+Z_e} \tag{3.8a}$$

$$\Gamma_{sd} = \frac{Z_s - Z_d}{Z_s + Z_d} \qquad \Gamma_{Ld} = \frac{Z_L - Z_d}{Z_L + Z_d} \tag{3.8b}$$

$$\theta_e = e^{-j\frac{\omega l}{v_e}} \tag{3.8c}$$

$$\theta_d = e^{-j\frac{\omega l}{v_d}} \tag{3.8d}$$

Equations (3.6) and (3.7) give the coefficients for the time harmonic periodic excitation where V_{s1} and V_{s2} are assumed to have the same frequency. From these equations it is seen that even or odd mode can be matched. Particularly, when $Z_s = Z_e$ and $Z_L = Z_d$, we have

$$A_e = \frac{(V_{s1} + V_{s2})}{4} \tag{3.9a}$$

$$B_e = \frac{-(V_{s1} + V_{s2})\theta_e^2 \Gamma_{Ld}^2}{4} \tag{3.9b}$$

$$A_d = \frac{(V_{s1} - V_{s2})Z_d}{2(Z_d + Z_e)} \tag{3.9c}$$

$$B_d = 0 \tag{3.9d}$$

In the case where the excitation is not periodic, contributions from all frequencies must be included in the general solution. The coefficients , thus become continuous functions of frequency. In the time domain, solutions for the voltages and currents are obtained by integrating over all frequencies. We therefore have

$$V_1(t,x) = \int_{-\infty}^{+\infty} A_e(\omega)\, e^{+j\omega t - \frac{x}{v_e}}\, d\omega + \int_{-\infty}^{+\infty} B_e(\omega)\, e^{+j\omega t + \frac{x}{v_e}}\, d\omega \tag{3.10a}$$

$$+\int_{-\infty}^{+\infty} A_d(\omega)\, e^{+j\omega\left(t-\frac{x}{v_d}\right)}\, d\omega + \int_{-\infty}^{+\infty} B_d(\omega)\, e^{+j\omega\left(t+\frac{x}{v_d}\right)}\, d\omega$$

$$I_1(t,x) = \frac{1}{Z_e}\int_{-\infty}^{+\infty} A_e(\omega)\, e^{+j\omega\left(t-\frac{x}{v_e}\right)}\, d\omega - \frac{1}{Z_e}\int_{-\infty}^{+\infty} B_e(\omega)\, e^{+j\omega\left(t+\frac{x}{v_e}\right)}\, d\omega \tag{3.10b}$$

$$+\frac{1}{Z_d}\int_{-\infty}^{+\infty} A_d(\omega)\, e^{+j\omega\left(t-\frac{x}{v_d}\right)}\, d\omega - \frac{1}{Z_d}\int_{-\infty}^{+\infty} B_d(\omega)\, e^{+j\omega\left(t+\frac{x}{v_d}\right)}\, d\omega$$

$$V_2(t,x) = \int_{-\infty}^{+\infty} A_e(\omega)\, e^{+j\omega\left(t-\frac{x}{v_e}\right)}\, d\omega + \int_{-\infty}^{+\infty} B_e(\omega)\, e^{+j\omega\left(t+\frac{x}{v_e}\right)}\, d\omega \tag{3.11a}$$

$$-\int_{-\infty}^{+\infty} A_d(\omega)\, e^{+j\omega\left(t-\frac{x}{v_d}\right)}\, d\omega - \int_{-\infty}^{+\infty} B_d(\omega)\, e^{+j\omega\left(t+\frac{x}{v_d}\right)}\, d\omega$$

$$I_2(t,x) = \frac{1}{Z_e}\int_{-\infty}^{+\infty} A_e(\omega)\, e^{+j\omega\left(t-\frac{x}{v_e}\right)}\, d\omega - \frac{1}{Z_e}\int_{-\infty}^{+\infty} B_e(\omega)\, e^{+j\omega\left(t+\frac{x}{v_e}\right)}\, d\omega \tag{3.11b}$$

$$-\frac{1}{Z_d}\int_{-\infty}^{+\infty} A_d(\omega)\, e^{+j\omega\left(t-\frac{x}{v_d}\right)}\, d\omega + \frac{1}{Z_d}\int_{-\infty}^{+\infty} B_d(\omega)\, e^{+j\omega\left(t+\frac{x}{v_d}\right)}\, d\omega$$

This can be rewritten in a simpler form as

$$V_1 = S_1 + S_2 + S'_1 + S'_2 \tag{3.12a}$$

$$I_1 = \frac{S_1}{Z_e} - \frac{S_2}{Z_e} + \frac{S'_1}{Z_d} - \frac{S'_2}{Z_d} \tag{3.12b}$$

$$V_2 = S_1 + S_2 - S'_1 - S'_2 \tag{3.13a}$$

$$I_2 = \frac{S_1}{Z_e} - \frac{S_2}{Z_e} - \frac{S'_1}{Z_d} + \frac{S'_2}{Z_d} \tag{3.13b}$$

where S_1, S_2, S'_1, and S'_2 are the forward and reflected voltage waves for the even and odd modes.

$$S_1 = \int_{-\infty}^{+\infty} A_e(\omega)\, e^{+j\omega t - \frac{x}{v_e}}\, d\omega \tag{3.14}$$

$$S_2 = \int_{-\infty}^{+\infty} B_e(\omega)\, e^{+j\omega t + \frac{x}{v_e}}\, d\omega \tag{3.15}$$

$$S'_1 = \int_{-\infty}^{+\infty} A_d(\omega)\, e^{+j\omega t - \frac{x}{v_d}}\, d\omega \tag{3.16}$$

$$S'_2 = \int_{-\infty}^{+\infty} B_d(\omega)\, e^{+j\omega t + \frac{x}{v_d}}\, d\omega \tag{3.17}$$

It is easy to recognize that the coefficients $A_e(\omega)$, $B_e(\omega)$, $A_d(\omega)$, and $B_d(\omega)$ are the Fourier transforms of S_1, S_2, S'_1 and S'_2 respectively. By applying the same boundary conditions as for the time harmonic case and keeping the assumption, $Z_{s1}=Z_{s2}=Z_s$ and $Z_{L1}=Z_{L2}=Z_L$, we can solve for these coefficients in the frequency domain

$$A_e(\omega) = \frac{[W_{s1}(\omega) + W_{s2}(\omega)]Z_e}{2(Z_e + Z_s)} \quad \frac{1}{1 - \Gamma_{se}\Gamma_{Le}\theta_e^2} \tag{3.18a}$$

$$B_e(\omega) = \frac{-[W_{s1}(\omega) + W_{s2}(\omega)]Z_e\Gamma_{Le}\theta_e^2}{2(Z_e + Z_s)} \quad \frac{1}{1 - \Gamma_{se}\Gamma_{Le}\theta_e^2} \tag{3.18b}$$

$$A_d(\omega) = \frac{[W_{s1}(\omega) - W_{s2}(\omega)]Z_e}{2(Z_e + Z_s)} \quad \frac{1}{1 - \Gamma_{sd}\Gamma_{Ld}\theta_d^2} \tag{3.19a}$$

$$B_d(\omega) = \frac{-[W_{s1}(\omega) - W_{s2}(\omega)]Z_d \Gamma_{Ld} \theta_d^2}{2(Z_d + Z_s)} \frac{1}{1 - \Gamma_{sd} \Gamma_{Ld} \theta_d^2} \tag{3.19b}$$

where $W_{s1}(\omega)$ and $W_{s2}(\omega)$ are the Fourier transforms of $V_{s1}(t)$ and $V_{s2}(t)$, respectively.

$$W_{s1}(\omega) = \frac{1}{2\pi} \int_{-\infty}^{+\infty} V_{s1}(t)\, e^{-j\omega t}\, dt \tag{3.20}$$

$$W_{s2}(\omega) = \frac{1}{2\pi} \int_{-\infty}^{+\infty} V_{s2}(t)\, e^{-j\omega t}\, dt \tag{3.21}$$

Since for passive terminations we always have

$$|\Gamma_{se} \Gamma_{Le} \theta_e^2| \leq 1 \tag{3.22}$$

and

$$|\Gamma_{sd} \Gamma_{Ld} \theta_d^2| \leq 1 \tag{3.23}$$

Equations (3.18) and (3.19) can be written in the form of infinite geometric series of the reflection coefficients.

$$A_e(\omega) = \frac{(W_{s1} + W_{s2})Z_e}{2(Z_e + Z_s)} \sum_{k=0}^{\infty} \Gamma_{se}^k \Gamma_{Le}^k\, e^{-2j\frac{\omega l}{v_e}} \tag{3.24a}$$

$$B_e(\omega) = -\frac{(W_{s1} + W_{s2})Z_e}{2(Z_e + Z_s)} \sum_{k=0}^{\infty} \Gamma_{se}^k \Gamma_{Le}^{k+1}\, e^{-2j\frac{\omega(k+1)l}{v_e}} \tag{3.24b}$$

$$A_d(\omega) = \frac{(W_{s1} - W_{s2})Z_d}{2(Z_d + Z_s)} \sum_{k=0}^{\infty} \Gamma_{sd}^k \Gamma_{Ld}^k \, e^{-2j\frac{\omega k l}{v_d}} \tag{3.25a}$$

$$B_d(\omega) = -\frac{(W_{s1} - W_{s2})Z_d}{2(Z_d + Z_s)} \sum_{k=0}^{\infty} \Gamma_{sd}^k \Gamma_{Ld}^{k+1} \, e^{-2j\frac{\omega (k+1) l}{v_d}} \tag{3.25b}$$

Using Equations (3.14) through (3.17) and making use of the time delay theorem for Fourier transforms, we can then invert for the associated modal voltage waves in the time domain.

$$S_1(t,x) = \frac{Z_e}{2(Z_e+Z_s)} \sum_{k=0}^{\infty} [V_{s1}(t - \frac{x+2kl}{v_e}) + V_{s2}(t - \frac{x+2kl}{v_e})] \, \Gamma_{se}^k \Gamma_{Le}^k \tag{3.26}$$

$$S_2(t,x) = \frac{-Z_e}{2(Z_e+Z_s)} \sum_{k=0}^{\infty} [V_{s1}(t + \frac{x-2(k+1)l}{v_e}) + V_{s2}(t + \frac{x-2(k+1)l}{v_e})] \, \Gamma_{se}^k \Gamma_{Le}^{k+1} \tag{3.27}$$

$$S'_1(t,x) = \frac{Z_d}{2(Z_d+Z_s)} \sum_{k=0}^{\infty} [V_{s1}(t - \frac{x+2kl}{v_d}) - V_{s2}(t - \frac{x+2kl}{v_d})] \, \Gamma_{sd}^k \Gamma_{Ld}^k \tag{3.28}$$

$$S'_2(t,x) = \frac{-Z_d}{2(Z_d+Z_s)} \sum_{k=0}^{\infty} [V_{s1}(t + \frac{x-2(k+1)l}{v_d}) - V_{s2}(t + \frac{x-2(k+1)l}{v_d})] \, \Gamma_{sd}^k \Gamma_{Ld}^{k+1} \tag{3.29}$$

and using relations (3.12) and (3.13), the voltages and currents on both lines can be obtained.

These equations show that the resulting signals on the lines can be expressed as an infinite sum of delayed and attenuated replicas of the the original applied voltages. They apply for arbitrary waveforms and allow to determine the voltage and current magnitudes at any time and any position along the lines. Convergence of the series depends on the reflection coefficient at the source and receiving ends. These relations also indicate that the difference in modal velocities of propagation can lead to abrupt changes in the signal waveforms. This is best illustrated in Fig. 3.2 where only line 1 is excited. For a reading at $x=0$ on line 2, the reflected even and odd mode signal (S_2 and S'_2) arrive at slightly

different times and since their contributions are of opposite signs (cf. Eq.(3.13a)), they produce an impulse in the waveform of line 2. Such a disturbance, however, does not occur in line 1 since S_2 and S'_2 are added according to (3.12a).

Experimental readings were performed using a PG502 Tektronix pulse generator and a microstrip pair (Figs. 3.2 and 3.3). The readings were found to verify the theory which can also be extended to describe complex terminations.

3.2 Capacitive Terminations

Most digital applications for transmission lines include devices such as diodes, transistors, and logic gates. Ideally the input impedance of such devices is very high and the input capacitance is minimized to insure small switching delays. In practice as rise and fall times become shorter, any small capacitance must be taken into consideration, this is more important when several identical devices are connected to the far end of a single microstrip line. Capacitance is related to the carriers in the devices ; for instance, in the case of a bipolar transistor, a diffusion capacitance associated with the charge store in the base and a transition capacitance related to the base-emitter space charge layer make up the total input capacitance. This suggests that the impedance seen is strongly nonlinear; however, an average capacitance can always be defined and used to implement a good linear model.

In the case where the load impedance consists of a resistor R, in parallel with a capacitor C, (Fig. 3.4a), the reflection coefficients Γ_{Le} and Γ_{Ld} for the even and odd modes in the frequency domain become functions of frequency.

$$\Gamma_{Le} = \frac{-\rho_e + j\omega\tau_e}{1 + j\omega\tau_e} \tag{3.30}$$

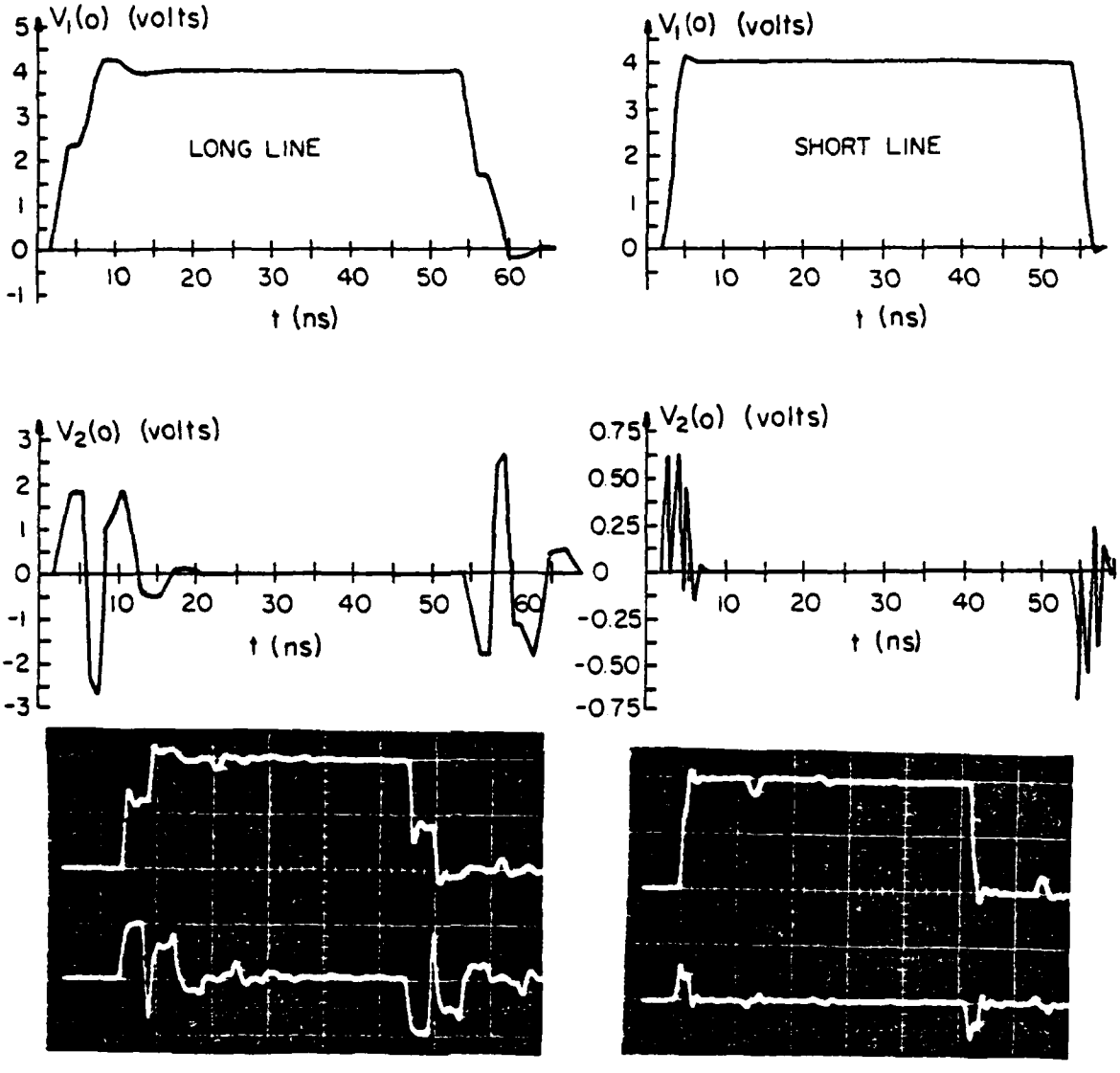

Figure 3.2 : Cross-coupling for passive terminations with far end opened. Theoretical (plots) and actual (photographs) waveforms for a long (left) and short (right) pair of coupled microstrip lines. Photographs : top waveforms are $V_1(0)$ (driving line) with vertical : 2 *V /div*, bottom waveforms are $V_2(0)$ (idle line) with vertical : 0.5 *V /div*. Each horizontal division is 5 *ns*. The spikes on the waveforms of $V_2(0)$ are due to the delay differences between odd and even mode reflections. For a short pair of lines, these spikes can no longer be detected by the scope because of their short duration.

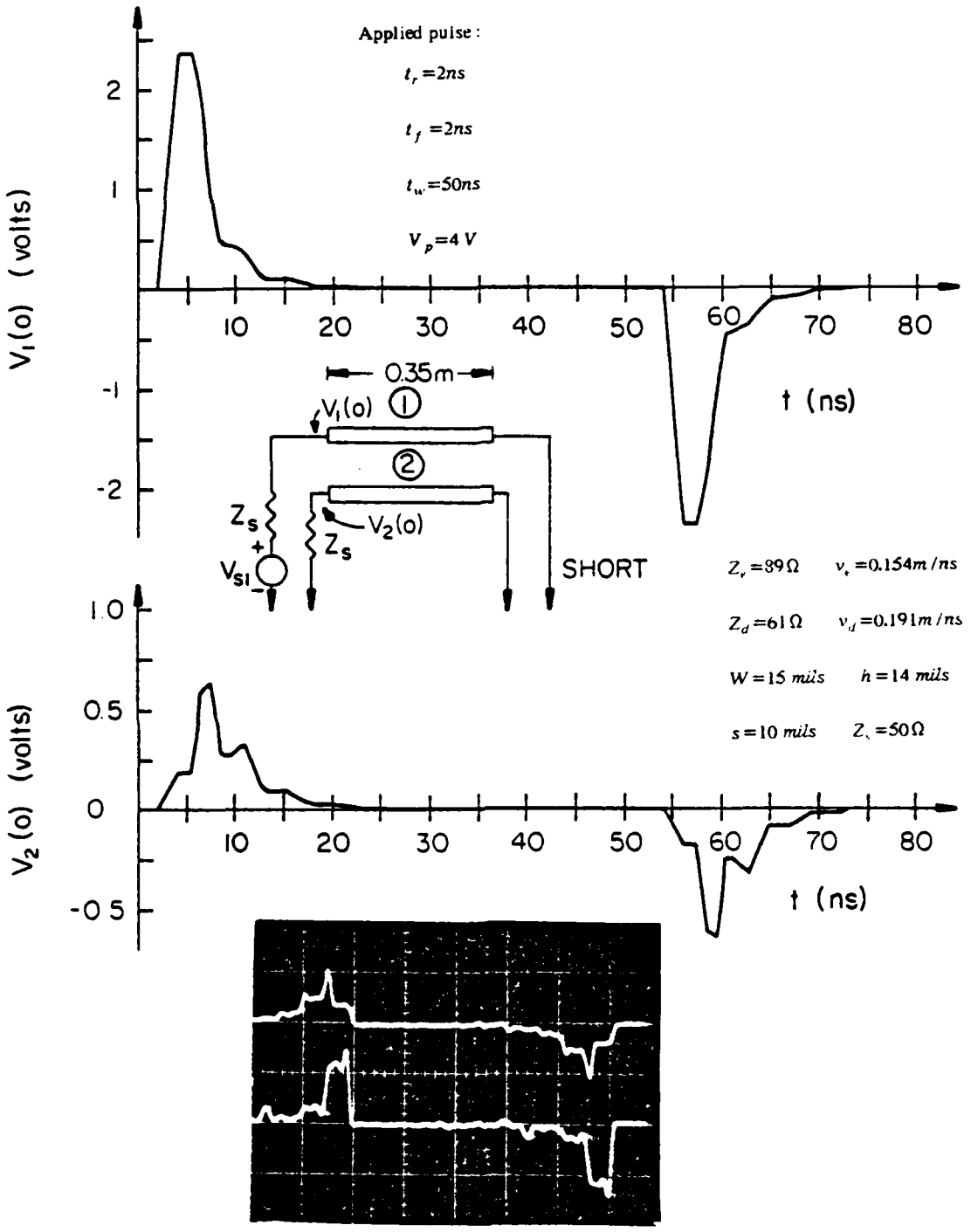

Figure 3.3 : Cross-coupling for passive terminations with far end shorted. Theoretical (plot) and actual (photograph) waveforms. Photographs : top waveform is $V_1(0)$ (driving line) with vertical ; 1 *V /div*, bottom waveform is $V_2(0)$ (idle or sense line) with vertical : 0.5 *V /div*. Each horizontal division is 5 *ns*.

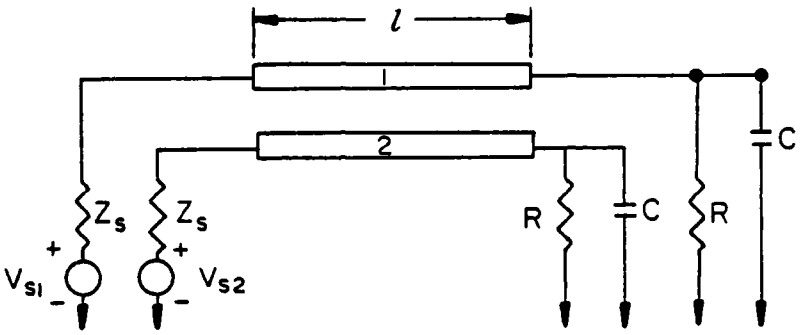

(a)

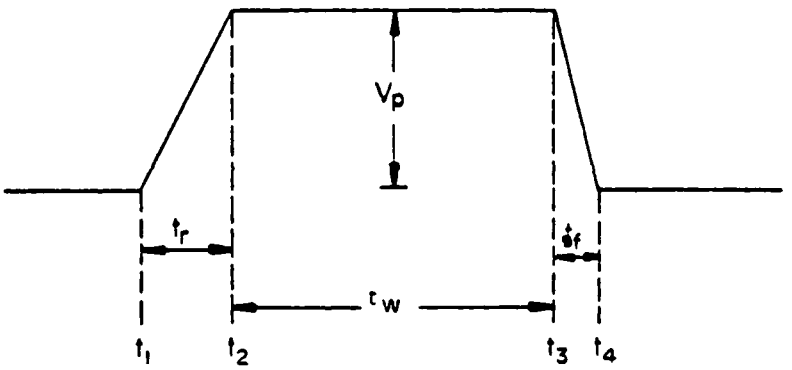

(b)

Figure 3.4 : (a) coupled microstrip lines with complex loads and (b) applied pulse.

$$\Gamma_{Ld} = \frac{-\rho_d + j\omega\tau_d}{1 + j\omega\tau_d} \tag{3.31}$$

where we have defined

$$\rho_e = \frac{R - Z_e}{R + Z_e} \qquad \tau_e = \frac{RZ_eC}{R + Z_e} \tag{3.32}$$

$$\rho_d = \frac{R - Z_d}{R + Z_d} \qquad \tau_d = \frac{RZ_dC}{R + Z_d} \tag{3.33}$$

Since Γ_{Le} and Γ_{Ld} are functions of frequency, the time domain solutions for the modal voltages are convolutions of the delayed source voltages and the inverse transforms of $\Gamma_{Le}(\omega)$ or $\Gamma_{Ld}(\omega)$.

$$S_1(t,x) = \frac{Z_e}{2(Z_e + Z_s)} \sum_{k=0}^{\infty}[V_{s1}(t - \frac{x + 2kl}{v_e}) + V_{s2}(t - \frac{x + 2kl}{v_e})]\Gamma_{se}^k * F^{-1}[\Gamma_{Le}^k(\omega)] \tag{3.34a}$$

$$S_2(t,x) = -\frac{Z_e}{2(Z_e + Z_s)} \sum_{k=0}^{\infty}[V_{s1}(t + \frac{x - 2(k+1)l}{v_e}) + V_{s2}(t + \frac{x - 2(k+1)l}{v_e})]\Gamma_{se}^k * F^{-1}[\Gamma_{Le}^{k+1}(\omega)] \tag{3.34b}$$

$$S'_1(t,x) = \frac{Z_d}{2(Z_d + Z_s)} \sum_{k=0}^{\infty}[V_{s1}(t - \frac{x + 2kl}{v_d}) - V_{s2}(t - \frac{x + 2kl}{v_d})]\Gamma_{sd}^k * F^{-1}[\Gamma_{Ld}^k(\omega)] \tag{3.35a}$$

$$S'_2(t,x) = -\frac{Z_d}{2(Z_d + Z_s)} \sum_{k=0}^{\infty}[V_{s1}(t + \frac{x - 2(k+1)l}{v_d}) - V_{s2}(t + \frac{x - 2(k+1)l}{v_d})]\Gamma_{sd}^k * F^{-1}[\Gamma_{Ld}^{k+1}(\omega)] \tag{3.35b}$$

where * denotes a convolution. Let us consider

$$\Gamma = \frac{-\rho + j\omega\tau}{1 + j\omega\tau} \tag{3.36}$$

The associated inverse Fourier transform is

$$F^{-1}[\Gamma(\omega)] = \left|\delta(t) - \left|\frac{1+\rho}{\tau}\right| u(t)\right| e^{\frac{-t}{\tau}} \tag{3.37}$$

where $u(t)$ is the unit step function and $\delta(t)$ is the unit impulse function. Finding the inverse transform of $\Gamma^k(\omega)$ implies applying the convolution theorem k times ; it can be shown that

$$F^{-1}\left|\Gamma^k(\omega)\right| = F^{-1}\left|\frac{-\rho + j\omega\tau}{1 + j\omega\tau}\right|^k = \left|\delta(t) + (-1)^k \sum_{j=0}^{k-1} D_{jk}\, t^j \left|\frac{1+\rho}{\tau}\right|^{j+1}\right| e^{\frac{-t}{\tau}} \tag{3.38}$$

where D_{jk} are constant coefficients satisfying the recursion relation

$$D_{0k} = k(-1)^{k-1} \qquad j=0 \tag{3.39a}$$

$$D_{jk} = -D_{j,k-1} + \frac{D_{j-1,k-1}}{j} \qquad j>0 \tag{3.39b}$$

so that Equations (3.34)-(3.35) become

$$S_1(t,x) = \frac{Z_e}{2(Z_e + Z_s)} \sum_{k=0}^{\infty} [V_{s1}(t - \frac{x + 2kl}{v_e}) + V_{s2}(t - \frac{x + 2kl}{v_e})]\Gamma_{se}^k * \left|\delta(t) + (-1)^k \sum_{j=0}^{k-1} D_{jk}\, t^j \left|\frac{1+\rho_e}{\tau_e}\right|^{j+1}\right| e^{\frac{-t}{\tau_e}} \tag{3.40a}$$

$$S_2(t,x) = -\frac{Z_e}{2(Z_e + Z_s)} \sum_{k=0}^{\infty} [V_{s1}(t + \frac{x - 2(k+1)l}{v_e}) + V_{s2}(t + \frac{x - 2(k+1)l}{v_e})]\Gamma_{se}^k *$$

$$\left[\delta(t) + (-1)^{k+1}\sum_{j=0}^{k-1} D_{j,k+1}\, t^{j} \left[\frac{1+\rho_e}{\tau_e}\right]^{j+1}\right] e^{\frac{-t}{\tau_e}} \qquad (3.40b)$$

$$S^{-}_{1}(t,x) = \frac{Z_d}{2(Z_d+Z_s)} \sum_{k=0}^{\infty}[V_{s1}(t - \frac{x+2kl}{v_d}) - V_{s2}(t - \frac{x+2kl}{v_d})]\Gamma_{sd}^{k} *$$

$$\left[\delta(t) + (-1)^{k} \sum_{j=0}^{k-1} D_{j,k}\; t^{j} \left[\frac{1+\rho_d}{\tau_d}\right]^{j+1}\right] e^{\frac{-t}{\tau_d}} \qquad (3.41a)$$

$$S^{-}_{2}(t,x) = -\frac{Z_d}{2(Z_d+Z_s)} \sum_{k=0}^{\infty}[V_{s1}(t + \frac{x-2(k+1)l}{v_d}) - V_{s2}(t + \frac{x-2(k+1)l}{v_d}]\Gamma_{sd}^{k} *$$

$$\left[\delta(t) + (-1)^{k+1}\sum_{j=0}^{k-1} D_{j,k+1}\, t^{j} \left[\frac{1+\rho_d}{\tau_d}\right]^{j+1}\right] e^{\frac{-t}{\tau_d}} \qquad (3.41b)$$

In the case where the applied excitation is a pulse (cf. Fig. 3.4b), $V_{s1}(t)$ and $V_{s2}(t)$ have the form

$$V_s(t) = \begin{cases} 0 & ; \quad t \leq 0 \\ V_p \dfrac{(t-t_1)}{(t_2-t_1)} & ; \quad t_1 \leq t \leq t_2 \\ V_p & ; \quad t_2 \leq t \leq t_3 \\ V_p \dfrac{(t-t_4)}{(t_3-t_4)} & ; \quad t_3 \leq t \leq t_4 \\ 0 & ; \quad t \geq t_4 \end{cases} \qquad (3.42)$$

Moreover, the convolution integral

$$I = \int_{0}^{(t-t_1)} \frac{(t-t_1-\lambda)}{(t_2-t_1)} V_p\, e^{-\frac{\lambda}{\tau}} \lambda^{j} d\lambda \qquad (3.43)$$

can be solved by using the j^{th} order derivative Theorem for Laplace transforms.

$$\int_0^{(t-t_1)} \lambda^j e^{-s\lambda} d\lambda = \left| \frac{j!}{s^{j+1}} - \sum_{m=0}^{j} \frac{m!}{s^{m+1}} (t-t_1)^{j-m} e^{-s(t-t_1)} \right| \tag{3.44}$$

Therefore, if we define

$$C = V_s(t) * \left| \delta(t) + (-1)^k \sum_{j=0}^{k-1} D_{jk} t^j \left| \frac{1+\rho}{\tau} \right|^{j+1} \right| e^{\frac{-t}{\tau}} \tag{3.45}$$

we have

$$C = V_s(t) + (-1)^{k-1} \sum_{j=0}^{k-1} D_{jk} t^j \left| \frac{1+\rho}{\tau} \right|^{j+1} \times \tag{3.46}$$

$$V_p \frac{(t-t_1)}{(t_2-t_1)} \left| j!\, \tau^{j+1} - \sum_{m=0}^{j} m!\, \tau^{m+1} e^{\frac{(t-t_1)}{\tau}} \right|$$

$$- (-1)^{k-1} \sum_{j=0}^{k-1} D_{jk} t^j \left| \frac{1+\rho}{\tau} \right|^{j+1} \times$$

$$\frac{V_p}{(t_2-t_1)} \left| (j+1)!\, \tau^{j+2} - \sum_{m=0}^{j} m!\, \tau^{m+1} (t-t_1)^{j-m+1} e^{-\frac{(t-t_1)}{\tau}} \right|$$

for $t_1 \leqslant t \leqslant t_2$

$$C = V_s(t) + (-1)^{k-1} \sum_{j=0}^{k-1} D_{jk} t^j \left| \frac{1+\rho}{\tau} \right|^{j+1} V_p \left| j!\, \tau^{j+1} - \sum_{m=0}^{j} m!\, \tau^{m+1} (t-t_2)^{j-m} e^{\frac{(t-t_1)}{\tau}} \right|$$

for $t_2 \leqslant t \leqslant t_3$

$$C = V_s(t) + (-1)^{k-1} \sum_{j=0}^{k-1} D_{jk} t^j \left| \frac{1+\rho}{\tau} \right|^{j+1} \times$$

$$V_p \frac{(t-t_3)}{(t_3-t_4)} \left| j!\,\tau^{j+1} - \sum_{m=0}^{j} m!\,\tau^{m+1}\, e^{-\frac{(t-t_3)}{\tau}} \right|$$

$$-(-1)^{k-1} \sum_{j=0}^{k-1} D_{j,k}\, t^j \left| \frac{1+\rho}{\tau} \right|^{j+1} \times$$

$$-\frac{V_p}{(t_3-t_4)} \left| (j+1)!\,\tau^{j+2} - \sum_{m=0}^{j} m!\,\tau^{m+1}\,(t-t_3)^{j-m+1}\, e^{-\frac{(t-t_3)}{\tau}} \right|$$

for $t_3 \leq t \leq t_4$

where we have made use of

$$f(t) * \delta(t)\, e^{-\alpha t} = f(t) \tag{3.47}$$

Using these relations in (3.40) and (3.41), we can obtain the expressions for the modal voltages. These equations can be easily implemented on a computer program to simulate the waveforms produced by a pulse. Such example is shown in Figs. 3.5 and 3.6. As expected the pulse width, the length of the lines, and the RC time constant are the most important parameters that determine the shape of the waveforms. As for the case of passive loads, fast pulses can result at the sending end of a quiet line, (waveshape of $V_2(0)$). These fluctuations cannot be observed accurately using presently available scopes since their duration is much shorter than the response of these instruments.

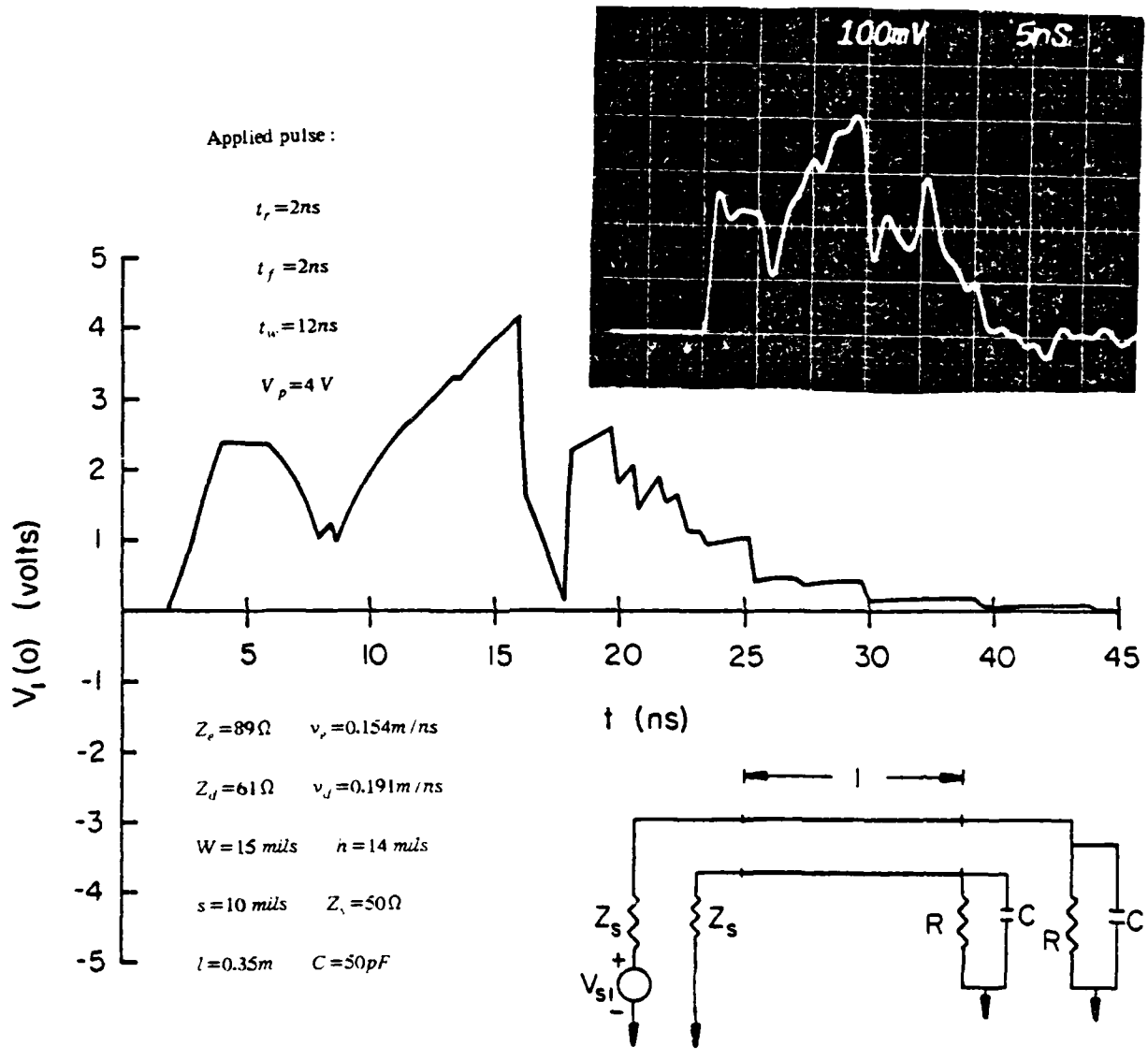

Figure 3.5 : Cross-coupling for capacitive loading. Theoretical (plot) and actual (photograph) waveforms of $V_1(0)$ (driving line). Photograph : voltage reading is attenuated by 10. R is infinite (open).

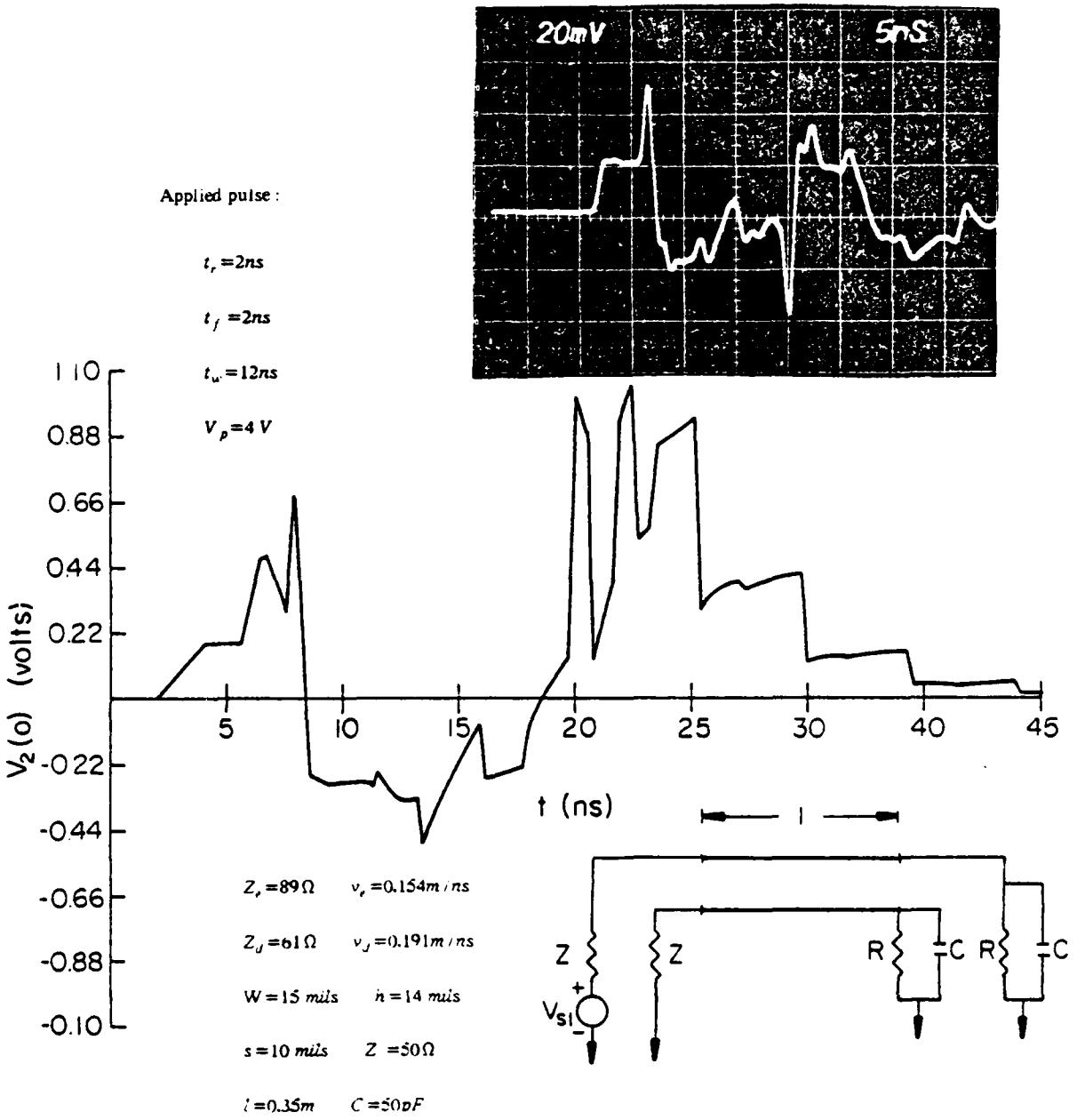

Figure 3.6 : Cross-coupling for capacitive loading. Theoretical (plot) and actual (photograph) waveform of $V_2(0)$ (idle line). Photograph : voltage reading is divided by 10. R is infinite (open).

CHAPTER 4

ANALYSIS OF MULTIPLE LINE STRUCTURES

The previous chapters dealt with with two microstrip line structures for which methods of measurements and time domain behavior were investigated. Structures consisting of more than two microstrip lines are, however, of greater occurrence in practical situations. In particular, the behavior of three-line systems in the frequency domain has been explored by several authors. Collier and El Deeb [29] have determined the scattering parameters for a six-port refectometer; Tripathi [30] derived expressions for the immitance parameters of symmetrical three-line microstrip circuits. Pavlidis and Hartnagel [31] derived the fundamental modes of propagations for these structures. Paul [32] constructed the matrix chain parameters for multiconductor transmission lines in the frequency domain. Pulse propagation however, requires a different and more complex analysis in the time domain. Fortunately, by using the insight gained in solving the two-line problems, expressions for multiple line structures in the time domain can be written *by inspection* provided that the different modes of propagation are identified. The goal of this chapter is to illustrate such an approach and generalize the techniques for n-line systems.

4.1 Three-Line Structures and Modes of Propagation

We first assume that the three microstrip lines shown in Fig. 4.1 are identical and that the two edge spacings are equivalent ; then the differential equations relating line voltages and currents can be written directly.

$$-\frac{\partial V_1}{\partial x} = L_{11}\frac{\partial I_1}{\partial t} + L_{12}\frac{\partial I_2}{\partial t} + L_{13}\frac{\partial I_3}{\partial t} \tag{4.1a}$$

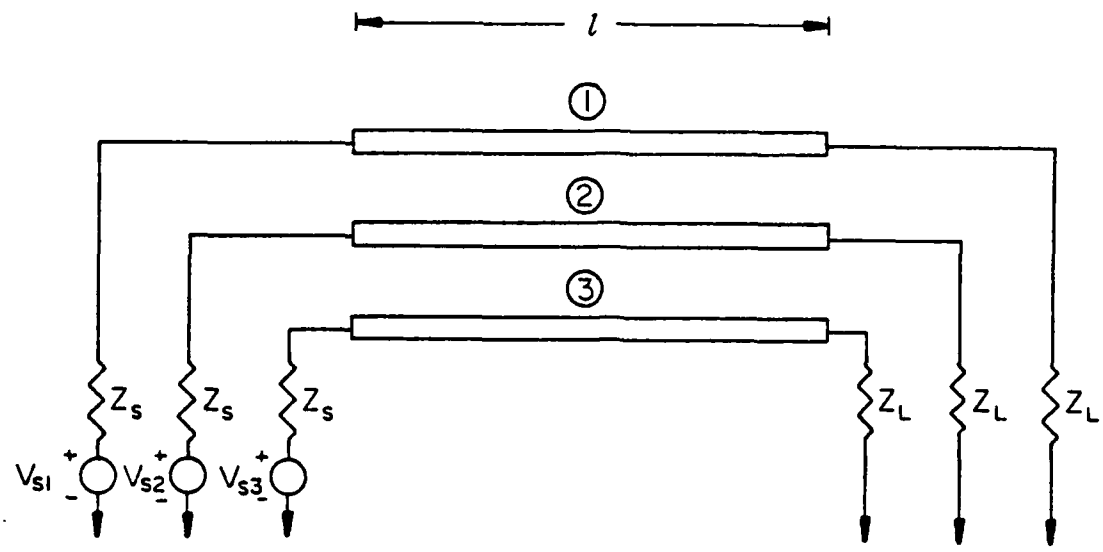

Figure 4.1 : Three-line coupler.

$$-\frac{\partial V_2}{\partial x} = L_{12}\frac{\partial I_1}{\partial t} + L_{11}\frac{\partial I_2}{\partial t} + L_{12}\frac{\partial I_3}{\partial t} \tag{4.1b}$$

$$-\frac{\partial V_3}{\partial x} = L_{13}\frac{\partial I_1}{\partial t} + L_{12}\frac{\partial I_2}{\partial t} + L_{11}\frac{\partial I_3}{\partial t} \tag{4.1c}$$

and

$$-\frac{\partial I_1}{\partial x} = C_{11}\frac{\partial V_1}{\partial t} + C_{12}\frac{\partial V_2}{\partial t} + C_{13}\frac{\partial V_3}{\partial t} \tag{4.2a}$$

$$-\frac{\partial I_2}{\partial x} = C_{12}\frac{\partial V_1}{\partial t} + C_{11}\frac{\partial V_2}{\partial t} + C_{12}\frac{\partial V_3}{\partial t} \tag{4.2b}$$

$$-\frac{\partial I_3}{\partial x} = C_{13}\frac{\partial V_1}{\partial t} + C_{12}\frac{\partial V_2}{\partial t} + C_{11}\frac{\partial V_3}{\partial t} \tag{4.2c}$$

where the $L_{i,j}$ and the $C_{i,j}$ are related to the physical parameters by

$$L_{11} = L_s \tag{4.3}$$

$$L_{12} = L_m \tag{4.4}$$

$$L_{13} = L_n \tag{4.5}$$

and

$$C_{11} = C_s + C_m + C_n \tag{4.6}$$

$$C_{12} = -C_m \tag{4.7}$$

$$C_{13} = C_n \tag{4.8}$$

The subscript m denotes mutual parameters between adjacent lines and the subscript n, mutual parameters between nonadjacent lines. If we define

$$V_o = V_1 - V_3 \tag{4.9a}$$

$$I_o = I_1 - I_3 \tag{4.9b}$$

we can determine a first mode of the system by subtracting (4.1c) from (4.1a) and (4.2c) from (4.2a). This yields

$$-\frac{\partial V_o}{\partial x} = (L_{11} - L_{13})\frac{\partial I_o}{\partial t} \tag{4.10a}$$

$$-\frac{\partial I_o}{\partial x} = (C_{11} - C_{13})\frac{\partial V_o}{\partial t} \tag{4.10b}$$

The velocity of propagation associated with this mode is

$$v_o = \frac{1}{\sqrt{(L_{11}-L_{13})(C_{11}-C_{13})}} = \frac{1}{\sqrt{(L_s-L_n)(C_s+C_m+2C_n)}} \tag{4.11}$$

Its characteristic impedance is

$$Z_o = \sqrt{\frac{L_{11} - L_{13}}{C_{11} - C_{13}}} = \sqrt{\frac{L_s - L_n}{C_s + C_m + 2C_n}} \tag{4.12}$$

A second mode can be obtained by defining

$$V_\xi = V_1 + \xi V_2 + V_3 \tag{4.13a}$$

$$I_\xi = I_1 + \xi I_2 + I_3 \tag{4.13b}$$

where ξ is a constant to be determined. When this linear combination is made using (4.1) and (4.2), we get

$$-\frac{\partial V_\xi}{\partial x} = (L_{11} + \xi L_{12} + L_{13})\frac{\partial I_1}{\partial t} \tag{4.14a}$$

$$+ (\frac{L_{12}}{\xi} + L_{11} + \frac{L_{12}}{\xi})\xi\frac{\partial I_2}{\partial t}$$

$$+ (L_{13} + \xi L_{12} + \xi L_{11})\frac{\partial I_3}{\partial t}$$

and

$$-\frac{\partial I_\xi}{\partial x} = (C_{11} + \xi C_{12} + C_{13})\frac{\partial V_1}{\partial t} \tag{4.14b}$$

$$+ (\frac{C_{12}}{\xi} + C_{11} + \frac{C_{12}}{\xi})\xi\frac{\partial I_2}{\partial t}$$

$$+ (C_{13} + \xi C_{12} + C_{11})\frac{\partial I_3}{\partial t}$$

We then introduce the approximations

$$L_{11} + \xi L_{12} + L_{13} \approx L_{11} + \xi L_{12} \tag{4.15}$$

$$C_{11} + \xi C_{12} + C_{13} \approx C_{11} + \xi C_{12} \tag{4.16}$$

which reduce Equation (4.14) to

$$-\frac{\partial V_\xi}{\partial x} = (L_{11} + \xi L_{12})\frac{\partial I_1}{\partial t} + (L_{11}+2\frac{L_{12}}{\xi})\xi\frac{\partial I_2}{\partial t} + (L_{11} + \xi L_{12})\frac{\partial I_3}{\partial t} \tag{4.17a}$$

$$-\frac{\partial I_\xi}{\partial x} = (C_{11} + \xi C_{12})\frac{\partial V_1}{\partial t} + (C_{11} + 2\frac{C_{12}}{\xi})\xi\frac{\partial V_2}{\partial t} + (C_{11} + \xi C_{12})\frac{\partial V_3}{\partial t} \tag{4.17b}$$

If we choose $\xi=+\sqrt{2}$, we then have

$$-\frac{\partial V_\xi}{\partial x} = (L_{11} + \sqrt{2}L_{12})\frac{\partial I_\xi}{\partial t} \tag{4.18}$$

$$-\frac{\partial I_\xi}{\partial x} = (C_{11} + \sqrt{2}C_{12})\frac{\partial V_\xi}{\partial t} \tag{4.19}$$

This pair of equations defines a second mode with propagation velocity

$$v_\xi = \frac{1}{\sqrt{(L_{11} + \sqrt{2}L_{12})(C_{11} + \sqrt{2}C_{12})}} = \frac{1}{\sqrt{(L_s + \sqrt{2}L_m)(C_s + C_n + (1-\sqrt{2})C_m)}} \tag{4.20}$$

and an associated wave impedance

$$Z_\xi = \sqrt{\frac{(L_{11} + \sqrt{2}L_{12})}{(C_{11} + \sqrt{2}C_{12})}} = \sqrt{\frac{(L_s + \sqrt{2}L_m)}{(C_s + C_n + (1-\sqrt{2})C_m)}} \tag{4.21}$$

Finally, a third mode is obtained in a similar manner by defining

$$V_\eta = V_1 + \eta V_2 + V_3 \tag{4.22a}$$

$$I_\eta = I_1 + \eta I_2 + I_3 \tag{4.22b}$$

Making the same approximations as per Equations (4.15) and (4.16) and setting $\eta = -\sqrt{2}$, we get

$$-\frac{\partial V_\eta}{\partial x} = (L_{11} - \sqrt{2})\frac{\partial I_\eta}{\partial t} \tag{4.23a}$$

$$-\frac{\partial I_\eta}{\partial x} = (C_{11} - \sqrt{2})\frac{\partial V_\eta}{\partial t} \tag{4.23b}$$

The propagation velocity is

$$v_\eta = \frac{1}{\sqrt{(L_{11} - \sqrt{2}L_{12})(C_{11} - \sqrt{2}C_{12})}} = \frac{1}{\sqrt{(L_s - \sqrt{2}L_m)(C_s + C_m + (1+\sqrt{2})C_m)}} \quad (4.24)$$

and the characteristic impedance is

$$Z_\eta = \sqrt{\frac{L_{11} - \sqrt{2}L_{12}}{C_{11} - \sqrt{2}C_{12}}} = \sqrt{\frac{L_s - \sqrt{2}L_m}{C_s + C_n + (1+\sqrt{2})C_m}} \quad (4.25)$$

The line variables can then be expressed in terms of the three modal variables as

$$V_1 = \frac{1}{2}\left|V_\alpha + \frac{V_\xi + V_\eta}{2}\right| \quad (4.26)$$

$$V_2 = \frac{V_\xi - V_\eta}{2\sqrt{2}} \quad (4.27)$$

$$V_3 = \frac{1}{2}\left|-V_\alpha + \frac{V_\xi + V_\eta}{2}\right| \quad (4.28)$$

and

$$I_1 = \frac{1}{2}\left|I_\alpha + \frac{I_\xi + I_\eta}{2}\right| \quad (4.29)$$

$$I_2 = \frac{I_\xi - I_\eta}{2\sqrt{2}} \quad (4.30)$$

$$I_3 = \frac{1}{2}\left|-I_\alpha + \frac{I_\eta + I_\eta}{2}\right| \quad (4.31)$$

It must be emphasized that these results apply if Equations (4.15) and (4.16) are valid. In general, such approximations are very well justified since in most cases $C_n << C_s + (1 \pm \sqrt{2})C_m$ and $L_n << L_s \pm \sqrt{2}L_m$. Figure 4.2 shows the different excitations associated with the three modes of the system in the case where the mutual coupling

$$Z = \sqrt{\frac{L_{11} + \sqrt{2}L_{12}}{C_{11} + \sqrt{2}C_{12}}}$$

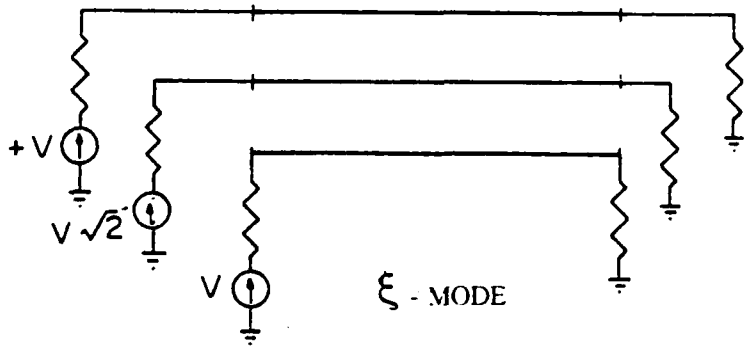

$$Z = \sqrt{\frac{L_{11} - \sqrt{2}L_{12}}{C_{11} - \sqrt{2}C_{12}}}$$

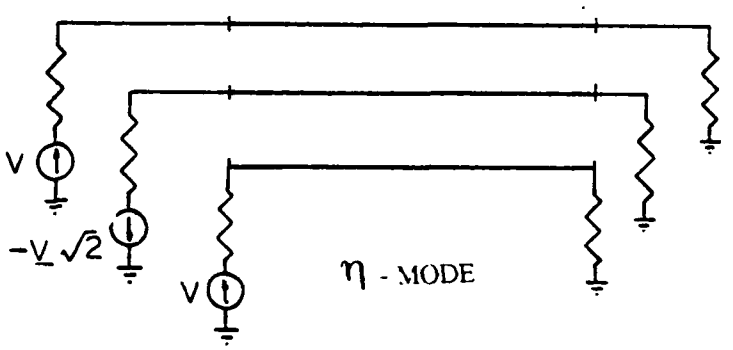

$$Z = \sqrt{\frac{L_{11}}{C_{11}}}$$

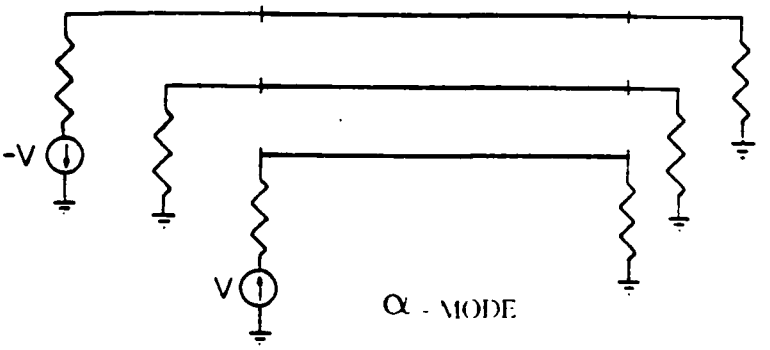

Figure 4.2 : Excitation of the three fundamental modes of a three-line coupler. It is assumed that the coupling between nonadjacent lines is negligible.

between nonadjacent lines is negligible. With the relations, derived, the general solution for the voltages and currents in the frequency domain can be established particularly for time harmonic excitation. By examining the two-line solutions, we can anticipate the general form for the three-line solutions, provided that the same assumptions regarding the terminations hold ; namely, $Z_{s1}=Z_{s2}=Z_{s3}=Z_s$, and $Z_{L1}=Z_{L2}=Z_{L3}=Z_L$. With this, we can write the modal voltages by inspection

$$V_{f\alpha} = A_\alpha \sum_{k=0}^{\infty}[V_{s1}(t - \frac{x+2kl}{v_\alpha}) - V_{s3}(t - \frac{x+2lk}{v_\alpha})]\,\Gamma_{s\alpha}^k\Gamma_{L\alpha}^k \tag{4.32a}$$

$$V_{b\alpha} = + B_\alpha \sum_{k=0}^{\infty}[V_{s1}(t + \frac{x-2(k+1)l}{v_\alpha} - V_{s3}(t + \frac{x-2(k+1)l}{v_\alpha})]\,\Gamma_{s\alpha}^k\Gamma_{L\alpha}^{k+1} \tag{4.32b}$$

$$V_{f\xi} = A_\xi \sum_{k=0}^{\infty}[V_{s1}(t - \frac{x+2kl}{v_\xi}) + \sqrt{2}V_{s2}(t - \frac{x+2kl}{v_\xi}) + V_{s3}(t - \frac{x+2kl}{v_\xi})]\,\Gamma_{s\xi}^k\Gamma_{L\xi}^{k+1} \tag{4.33a}$$

$$V_{b\xi} = B_\xi \sum_{k=0}^{\infty}[V_{s1}(t + \frac{x-2(k+1)l}{v_\xi}) + \sqrt{2}V_{s2}(t + \frac{x-2(k+1)l}{v_\xi}) + V_{s3}(t + \frac{x-2(k+1)l}{v_\xi})]\,\Gamma_{s\xi}^k\Gamma_{L\xi}^{k+1} \tag{4.33b}$$

$$V_{f\eta} = A_\eta \sum_{k=0}^{\infty}[V_{s1}(t - \frac{x+2kl}{v_\eta}) - \sqrt{2}V_{s2}(t - \frac{x+2kl}{v_\eta}) + V_{s3}(t + \frac{x+2kl}{v_\eta})]\,\Gamma_{s\eta}^k\Gamma_{L\eta}^k \tag{4.34a}$$

$$V_{b\eta} = B_\eta \sum_{k=0}^{\infty}[V_{s1}(t + \frac{x-2(k+1)l}{v_\eta}) - \sqrt{2}V_{s2}(t + \frac{x-2(k+1)l}{v_\eta}) + V_{s3}(t + \frac{x-2(k+1)l}{v_\eta})]\,\Gamma_{s\eta}^k\Gamma_{L\eta}^{k+1} \tag{4.34b}$$

where

$$\Gamma_{s\alpha} = \frac{Z_\alpha - Z_s}{Z_\alpha + Z_s} \qquad \Gamma_{L\alpha} = \frac{Z_\alpha - Z_L}{Z_\alpha + Z_L} \tag{4.35}$$

$$\Gamma_{s\xi} = \frac{Z_\xi - Z_s}{Z_\xi + Z_s} \qquad \Gamma_{L\xi} = \frac{Z_\xi - Z_L}{Z_\xi + Z_L} \tag{4.36}$$

$$\Gamma_{s\eta} = \frac{Z_\eta - Z_s}{Z_\eta + Z_s} \qquad \Gamma_{L\eta} = \frac{Z_\eta - Z_L}{Z_\eta + Z_L} \tag{4.37}$$

The modal voltages are as defined by Equations (4.9), (4.13), and (4.22) where the subscript f denotes a forward moving wave and b, a backward moving wave. Using (4.26)-(4.31), the line variables can be obtained. If we apply the boundary conditions at $x=0$ and at $x=l$, we get

$$A_\alpha = -B_\alpha = \frac{Z_\alpha}{Z_\alpha + Z_s} \tag{4.38}$$

$$A_\xi = -B_\xi = \frac{Z_\xi}{Z_\xi + Z_s} \tag{4.39}$$

$$A_\eta = -B_\eta = \frac{Z_\eta}{Z_\eta + Z_s} \tag{4.40}$$

4.2 N-Line Structures and Generalization

From the analysis performed, we can anticipate that n-line systems have solutions analogous to three-line structures. More precisely, if the terminations are identical, an expression can be written for the n-line structure from the modal characteristics. Since a matrix representation is more convenient, the problem involves the determination of the eigenvalues and eigenvectors which can be obtained using some approximations. The Telegraph Equations then become

$$-\frac{\partial^2 V}{\partial x^2} = LC\frac{\partial^2 V}{\partial t^2} \tag{4.41}$$

where L and C are $n \times n$ matrices and V a $n \times 1$ matrix for the line voltages. If the n modes of the system can be found, we can define an eigenvector matrix E such that

$$V_m = E\ V \tag{4.42}$$

V_m is the column matrix for the n modal voltages. The solution in terms of E and the matrix associated with the voltage sources at $x = 0$, V_s, is

$$V_{fm} = A_m \sum_{k=0}^{\infty} E\ \Gamma_{sm}^k \Gamma_{Lm}^k\ V_s(u_{fm}) \tag{4.43a}$$

$$V_{bm} = -A_m \sum_{k=0}^{\infty} E\ \Gamma_{sm}^k \Gamma_{Lm}^{k+1} V_{bm}(u_{bm}) \tag{4.43b}$$

where V_{fm} and V_{bm} are the modal voltage matrices for the forward and backward waves, respectively. A_m, Γ_{sm}, and Γ_{Lm} are diagonal $n \times n$ matrices associated with the source and load impedances and the corresponding mode ; u_{fm} and u_{bm} are the arguments associated with the mode m for forward and backward variables, respectively

$$u_{fm} = t - \frac{x + 2kl}{v_m} \qquad u_{bm} = t + \frac{x - 2(k+1)l}{v_m} \tag{4.44}$$

where v_m is the propagation velocity for mode m. From these relations, the line voltages can be found by applying

$$V = E^{-1}\left|V_{fm} + V_{bm}\right| \tag{4.45}$$

We then observe that the problem of finding the signal magnitudes at any time or any position of an n-line structure becomes that of finding the eigenvalues and the eigenvector

associated with the system. For a large number of lines, this problem becomes nontrivial however, by using computer routines or by setting some approximations such as those in Equations (4.15)-(4.16), one can arrive at satisfactory results. For instance, it can be assumed that mutual parameters associated with any two nonadjacent lines are negligible. This generates L and C matrices with only principal and secondary diagonal elements and facilitates the analytical or computer task.

The solution to n-line pulse driven structures applies to many digital network problems. When n logic gates are switching n other gates via transmission lines, noise and reflections induced on a quiet line can be determined at any point. This would provide margins for the applied signals (magnitude, pulse width, rise and fall times), and the microstrip line geometries (spacing, width, and dielectric constant).

CHAPTER 5

CONCLUSION

This study explored some of the problems associated with two-line structures and attempted a generalization to multiple line systems. These analyses represent the first steps for the investigation of more complex situations involving nonlinearities, capacitive terminations, and discontinuities along the lines. N-line systems with arbitrary terminations can therefore be treated using a numerical approach to provide reliable design guidelines for digital networks.

REFERENCES

[1] H. A. Wheeler, "Transmission Line Properties of Parallel Wide Strips by a Conformal Mapping Approximation," *IEEE Trans. Microwave Theory Tech.*, vol. MTT-12, pp. 280-288, May 1964.

[2] H. A. Wheeler, "Transmission Line Properties of Parallel Strips Separated by a Dielectric Sheet," *IEEE Trans. Microwave Theory Tech.*, vol. MTT-13, pp. 172-185, March 1965.

[3] P. Silvester, "TEM Wave Properties of Microstrip Transmission Lines," *Proc. IEEE* vol. 115, pp. 43-48, January 1968.

[4] T. G. Bryant and J. A. Weiss, "Parameters of Microstrip Transmission Lines and of Coupled Pairs of Microstrip Lines," *IEEE Trans. Microwave Theory Tech.*, vol. MTT-10, pp. 1021-1027, December 1968.

[5] A. Farrar and A. T. Adams, "A Potential Theory Method for Covered Microstrip," *IEEE Trans. Microwave Theory Tech.*, vol. MTT-21, pp. 494-496, July 1973.

[6] "Characteristic Impedance of Microstrip by the Method of Moments," *IEEE Trans. Microwave Theory Tech.*, vol. MTT-18, pp. 65-66, January 1970.

[7] E. Yamashita and R. Mittra, "Variational Method for the Analysis of Microstrip Lines," *IEEE Trans. Microwave Theory Tech.*, vol. MTT-16, pp. 251-256, April 1968.

[8] E. Yamashita, "Variational Method for the Analysis of Microstrip-Like Transmission Lines," *IEEE Trans. Microwave Theory Tech.*, vol. MTT-16, pp. 529-539, August 1968.

[9] M. V. Schneider, "Microstrip Lines For Microwave Integrated Circuits," *Bell Syst. Tech. J.*, vol. 48, pp. 1421-1444, May-June 1969.

[10] E. O. Hammerstad, "Equations for Microstrip Circuit Design," *Proc. European Microwave Conference, Hamburg (Germany)*, pp. 268-272, September 1975.

[11] W. J. Chudobiak et al., "Dispersion in Microstrip," *IEEE Trans. Microwave Theory Tech.*, vol. MTT-19, pp. 791-794, September 1971.

[12] W. J. Getsinger, "Microstrip Dispersion Model," *IEEE Trans. Microwave Theory Tech.*, vol. MTT-21, pp. 34-39, January 1973.

[13] R. P. Owens, "Predicted Frequency Dependence of Microstrip Characteristic Impedance Using the Planar-Waveguide Model," *Electron. Lett.*, vol. 12, pp. 269-270, May 27, 1976.

[14] J. D. Krauss and K. R. Carver, *Electromagnetics*. New York, NY : Mc Graw-Hill Book Company, Inc., 1973.

[15] "Time Domain Reflectometry," *Hewlett-Packard Journal*, vol. 15, no. 6, February 1964.

[16] "S-Parameter Design," *Hewlett-Packard Application Note 154*, April 1972.

[17] G. D. Vendelin, *Design of Amplifiers and Oscillators by the S-Parameter Method*. New York, NY ; John Wiley and Sons, 1982.

[18] B. M. Oliver, "Directional Electromagnetic Couplers," *Proc. IRE*, vol. 42, pp. 1686-1692, November 1954.

[19] D. W. Kammler, "Calculations of Characteristic Admittances and Coupling Coefficients for Strip Transmission Lines," *IEEE Trans. Microwave Theory Tech.*, vol. MTT-16 , pp. 925-937, November 1968.

[20] M. K. Krage and G. I. Haddad, "Characteristics of Coupled Microstrip Transmission Lines-I : Coupled Mode Formulation of Inhomogeneous Lines ," *IEEE Trans. Microwave Theory Tech.*, vol. MTT-18, pp. 217-222, April 1970.

[21] M. K. Krage and G. I. Haddad, "Characteristics of Coupled Microstrip Transmission Lines - II : Evaluation of Coupled Line Parameters," *IEEE Trans. Microwave Theory Tech.*, vol. MTT-18, pp. 222-228, April 1970.

[22] T. J. Bryant and J. A. Weiss, "Parameters of Microstrip Transmission Lines and of Coupled Pairs of Microstrip Lines," *IEEE Trans. Microwave Theory Tech.*, vol. MTT-16, no. 12, pp. 1021-1027, December 1968.

[23] R. Garg and I. J. Bahl "Characteristics of Coupled Microstrip Lines," *IEEE Trans. Microwave Theory Tech.*, vol. MTT-27, pp. 700-705, July 1979.

[24] E. Hammerstad and O. Jensen, "Accurate Models for Microstrip Computer-Aided Design," *IEEE MTT-S Int. Microwave Symp. Dig. (Washington,DC)*, 1980, pp. 407-409.

[25] Kirshing and R. Jensen, "Accurate Wide-Range Design Equations for the Frequency-Dependent Characteristics of Parallel Coupled Microstrip Lines," *IEEE Trans. Microwave Theory Tech.*, vol. MTT-32, pp. 83-90, January 1984.

[26] M. Cotte, "Theorie de la propagation d'ondes de choc sur deux lignes paralleles," *Revue Generale de l'Electricite*, pp. 343-352, August 1947.

[27] I. Catt, "Crosstalk (Noise) in Digital Systems," *IEEE Trans. Electronic Computers*, vol. EC-16, pp. 743-763, December 1967.

[28] D. B. Jarvis, "The Effects of Interconnections on High-Speed Logic Circuits," *IEEE Trans. Electronic Computers*, vol. EC-12, pp. 476-487, October 1963.

[29] R. Collier and N. El Deeb, "On the Use of a Microstrip Three-Line System as a Six-Port Reflectometer," *IEEE Trans. Microwave Theory Tech.*, vol. MTT-27, pp. 847-843, October 1979.

[30] V. K. Tripathi, "On the Analysis of Symmetrical Three-Line Microstrip Circuits," *IEEE Trans. Microwave Theory Tech.*, vol. MTT-25, pp. 726-729, September 1977.

[31] D. Pavlidis and H. Hartnagel, "The Design and Performance of Three-Line Microstrip Couplers," *IEEE Trans. Microwave Theory Tech.*, vol. MTT-25, pp. 631-640, October 1976.

[32] C. R. Paul, "Useful Matrix Chain Parameter Identities for the Analysis of Multiconductor Transmission Lines," *IEEE Trans. Microwave Theory Tech.*, vol. MTT-23, pp. 756-760, September 1975.

END

FILMED

1-86

DTIC